REPORT DOCUMENTATION PAGE

Form Approved
OMB NO. 0704-0188

1. AGENCY USE ONLY (Leave Blank)	2. REPORT DATE	3. REPORT TYPE AND DATES COVERED
		Final: 2/4/94 - 2/3/98

4. TITLE AND SUBTITLE
Measurement of Mean Wind Profiles and Spatial Gradients of the Mean Wind with the Volume Imaging Lidar

5. FUNDING NUMBERS
DAAH04-94-G-0022

6. AUTHOR(S)
Edwin W. Eloranta, Principal Investigator

7. PERFORMING ORGANIZATION NAME(S) AND ADDRESS(ES)
Department of Atmospheric and Oceanic Sciences
University of Wisconsin-Madison, 1225 West Dayton, Madison WI 53706

8. PERFORMING ORGANIZATION REPORT NUMBER

9. SPONSORING / MONITORING AGENCY NAME(S) AND ADDRESS(ES)
U. S. Army Research Office
P.O. Box 12211
Research Triangle Park, NC 27709-2211

10. SPONSORING / MONITORING AGENCY REPORT NUMBER
ARO 30961.7-EV

11. SUPPLEMENTARY NOTES
The views, opinions and/or findings contained in this report are those of the author(s) and should not be construed as an official Department of the Army position, policy or decision, unless so designated by the documentation.

12 a. DISTRIBUTION / AVAILABILITY STATEMENT
Approved for public release; distribution unlimited.

12 b. DISTRIBUTION CODE

13. ABSTRACT (Maximum 200 words)

The University of Wisconsin Volume Imaging Lidar was modified to increase the laser repetition rate from 30 to 100 Hz and to increase the resolution and dynamic range of the recorded signals. The modified system was used to observe cold air flows over Lake Michigan during the winter. These data, analyzed with improved algorithms for measuring wind velocities from the motions of aerosol inhomogeneities, have provided spatially resolved velocity, divergence and vorticity maps with a spatial resolution of 250 meters covering areas of greater than 50 square kilometers.

14. SUBJECT TERMS			15. NUMBER OF PAGES
			16. PRICE CODE
17. SECURITY CLASSIFICATION OR REPORT	18. SECURITY CLASSIFICATION ON THIS PAGE	19. SECURITY CLASSIFICATION OF ABSTRACT	20. LIMITATION OF ABSTRACT
UNCLASSIFIED	UNCLASSIFIED	UNCLASSIFIED	UL

NSN 7540-01-280-5500

Standard Form 298 (Rev.2-89)
Prescribed by ANSI Std. 239-18
298-102

19981222 042

Final Report

Measurement of Mean Wind Profiles and Spatial Gradients of the Mean Wind with the Volume Imaging Lidar

UW 144-DZ20
DAAH04-94-G-0022

E.W.Eloranta
Principal Investigator

University of Wisconsin
Dept. of Atmospheric and Oceanic Sciences
1225 W. Dayton St.
Madison,Wis
Tel (608)-262-7327

Table of Contents

1	Introduction	1
2	Lidar observations during Lake-ICE	2
3	Preliminary data analysis	3
4	Wind measurement algorithms	3
5	Sample data from lake-ICE	5
6	Preliminary LES modeling	15
7	References	18
8	Degrees based on ARO supported work	18
9	Personnel supported	19
10	Journal papers	19
11	Conference presentations	19
12	Appendices-conference abstracts	20
13	12th Symposium on Boundary Layers and Turbulence	21
14	13th Symposium on Boundary Layers and Turbulence	24
15	13th Symposium on Boundary Layers and Turbulence	29
16	19th-International Laser Radar Conference	35
17	19th-International Laser Radar Conference	39
18	4th-International Symposium on Tropospheric Profiling	46

1 Introduction

During the course of this grant the University of Wisconsin Volume Imaging Lidar (VIL) has been modified to substantially improve performance. Observations with the system are always faced with a trade-off between the need to scan a large volume quickly and the need for high spatial resolution. The maximum scan rate is limited by the repetition rate of the laser. With support from this grant and an Air Force contract we have increased the repetition rate of the lidar from 30 Hz to 100 Hz while also increasing the average transmitted power from 30 to 40 W. This required a new laser, faster computers, and a faster optical disk storage system. Both the front end computer which controls realtime aspects of the system and the host computer were replaced. It also required extensive modification to the control and image display software. The new data system provides sufficient bandwidth to accommodate the increased repetition rate and to increase the number of data points recorded per laser profile from 1024 to 1200. This allows an 18 km profile to be recorded at maximum resolution of 15 m/point instead of 15.3 km with the old data system. During previous field campaigns, we have experienced problems with maintaining alignment of the transmitting laser and the receiving telescope. This required the receiving telescope to operate with a larger than necessary angular field-of-view which increased the background sky light and thus decreased the signal-to-noise ratio. The optical subsystem which directs light to the atmosphere was redesigned to eliminate the mechanical instabilities which caused this problem. To further improve the signal quality the 10-bit digitizer used previously was replaced with a 12-bit model and a new logarithmic amplifier was designed. This new logarithmic amplifier increased the receiver dynamic range from 80 dB to 95 dB. Figure 1 presents a schematic drawing of the current VIL.

During the December of 1997 and January of 1998 the Volume Imaging Lidar was operated on the shore of Lake Michigan at Sheboygan, Wisconsin. Preparation for this experiment and December 1997 operations were supported by this grant. The remaining field deployment was funded under NSF grant ATM-9707165 as part of the Lake Induced Convection Experiment (Lake-ICE). NSF funding did not arrive until January of 1998. Work on preparing the Volume Imaging Lidar began in April of 1997. Our lidar measurements were designed to test the performance of Large Eddy Simulations (LES). The flow of cold wintertime air over the warm lake produces a convective boundary layer which grows in depth as a function of distance from the shore in response to heat input from a relatively uniform lake surface. This provides an ideal situation to test LES models. Ideally, the stable boundary layer leaving the shoreline does not contain large convective eddies and this would eliminate the need for cyclical boundary conditions in the offshore direction. The nearly steady state conditions also reduce the simulation time required because equilibrium is reached in approximately the time required for an air parcel to advect though the model domain. For this case equilibrium is reached in approximately 10 minutes, whereas typical afternoon boundary layer simulations require the model to simulate several hours of boundary layer development.

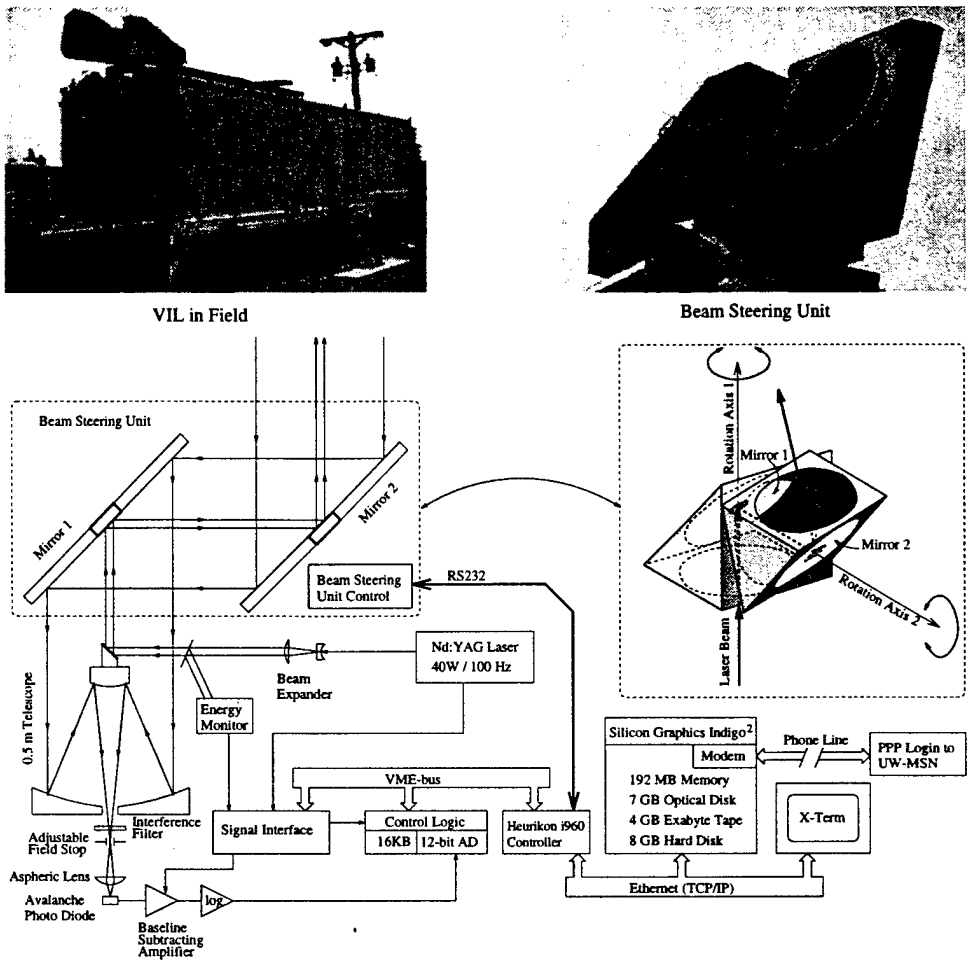

Figure 1. The Volume Imaging Lidar and a current hardware schematic.

The comprehensive analysis of this data is just beginning. Because results have not appeared in journal publications, this report includes examples of our preliminary data analysis. These analysis have produced spatial fields of the vector winds, divergence and vorticity having spatial resolutions of $\sim$ 250 m and covering an area of $\sim$ 100 km^2. The resolution and fidelity of even these preliminary results appear superior to that which has been obtained in any previous measurement by any technique.

2 Lidar observations during Lake-ICE

The University of Wisconsin Lidar Volume Imaging Lidar (VIL) was deployed on the shore of Lake Michigan as part of the Lake-ICE experiment. Approximately 40 giga-bytes of data were acquired during 45 hours of operation on 9 days between December 5, 1997 and January 19, 1998. The VIL performed well. Only minor difficulties with the laser cooling unit and the beam steering unit were experienced until near the end of the experiment. Optical damage to a laser rod required us to terminate operation one day before the end of Lake-ICE.

The VIL depicts atmospheric structure by sensing spatial inhomogeneities in aerosol backscattering. Prior to the experiment we were concerned that the aerosol content might be very low during Lake-ICE making it difficult to detect structure. These fears proved groundless and good conditions were present throughout the experiment. Nearly every day provided new and interesting data. Many days provided usable data thought the 18 km range of the recorded profiles.

The winter of 1997-98 was one of the warmest on record. However, the mild cold-air outbreaks provided sufficient temperature contrast with the lake to form internal boundary layers in the offshore flow. Preliminary analysis of our lidar observations suggest that these cases are suitable for evaluating the performance of Large-Eddy-Simulations. In addition to the expected internal boundary layer cases, the data set includes observations of a land-breeze circulation, complex gravity wave fields, and patterns of snow fall from thin lake-generated stratus clouds. Additional information on the VIL observations is provided in conference abstracts attached to this report.

The only major disappointment of the experiment, was our failure to acquire data from surface heat flux data buoys. This data would have been very useful in our LES modeling effort. The research group working on this project anchored two buoys in our scan area. Both stopped transmitting shortly after deployment. Attempts to recover the buoys were unsuccessful and these valuable instruments were lost. It appeared that the buoys had either broken loose from their anchors or sunk.

3 Preliminary Data Analysis

We have documented observation times and scan geometries for all VIL Lake-ICE data. In addition, MPEG animations have been created for all lidar scans. The data catalog and the MPEG animations are posted on our web page (http://lidar.ssec.wisc.edu, *Results from Lake-ICE*). This web site also includes MPEG animations of visible, infrared and water vapor imagery from the GOES satellite. Background information and photos depicting our participation in Lake-ICE are also presented. Time-resolved 2-d wind fields have been generated for the land-breeze case observed on December 21, 1997. Animations of these winds are also posted on our web page.

4 Wind Measurement Algorithms

In previous work we have developed algorithms to measure vertical profiles of the horizontal wind from volumetric lidar images of aerosol structure (Schols and Eloranta 1992, Piironen and Eloranta, 1995). These algorithms derived a single wind vector for each altitude representing the mean wind averaged over the ~ 100 km^2 area of a typical lidar scan. Under this grant we have been extended these algorithms to allow computation of the spatial variation of winds from successive azimuthal scans.

Wind processing follows the basic approach described by Piironen and Eloranta (1995). The only difference in the initial processing occurs because the scan consists of a single horizontal plane instead of a volume scan. The initial processing steps proceeds as follows:

1. Individual lidar shots are corrected for the r^{-2} dependence in lidar equation and then filtered with a running median hi-pass filter. The filter length was set to 450 m for the results presented in this report.

2. Next the lidar data is mapped to a Cartesian grid with a uniform spatial resolution of 15 meters. Data points on the Cartesian grid are computed from a linear interpolation between the 4 nearest points in the polar coordinates of the raw lidar profiles. To correct for the distortion of the lidar image caused by the wind, and a finite scan duration, the position of data points in the lidar profiles are adjusted to where to point they occupied at the time the first profile of the scan was acquired. The wind vector needed for this adjustment is estimated from a first trial solution and then the results of this solution are used for this distortion correction in final wind solution.

3. A temporal-median image is then formed from the complete set of Cartesian scan images. In order to remove station features and artifacts caused by attenuation, this median image is subtracted from each of the scan images.

4. Finally, to prevent individual bright features in the image from dominating the cross correlation function, the resulting images are subjected to a histogram normalization.

Up to this point the wind processing is nearly identical to the scheme for computing winds averaged over the entire scan area as described in Piironen and Eloranta. However, in order to compute the spatial varaition of the wind field, the scan area must now be divided into smaller sub-areas. Two-dimensional lag cross correlations are computed between successive scans in each of the sub-areas. These cross correlation functions are then averaged over a series of scan pairs. Wind vectors are then computed from the lag positions of averaged correlation function maximums and the time separation between scans.

In the computations presented below, winds are calculated in square sub-areas which are 250 meters on a side. Correlations are computed between every other scan so that left-right/right-left scans are always paired with the same scan direction and thus the time interval between laser profiles in each part of successive images is approximately the same. This results in a $\sim$ 24 sec time separation between scans. Because the winds were as large as 9 m/s, the wind advected structures by up to 216 meters between scans. This causes a problem with the cross correlation calculation because most of the structure seen in a sub-area in one scan has advected out of the sub-area by the time of the next scan. This creates small correlation maxima contaminated by random correlations between unrelated structures. To minimize this problem the correlation calculation is modified. The location of the sub-area in the second frame of each pair is displaced downwind by the distance the structure is expected to move between frames. This allows the correlation to take place with approximately the same features that were present in the first frame. The position of the

correlation maximum is then corrected for the displacement of the box to compute the wind vector. An estimate of the wind vector is required in order to select the displacement for the sub-area in the second frame. This is computed by first generating a lower resolution wind field where the advection distance is a smaller fraction of the sub-area's size. For the winds shown below, the wind field was first calculated in square sub-areas with sides of 500 m. The 500 m values were then used to compute displacements for the four 250 m areas in each of the larger areas.

5 Sample data from Lake-ICE

5.1 Data from January 13, 1998

Figure 2 shows the lidar backscatter structure observed on a horizontal plane 5 m above Lake Michigan's surface on January 13, 1998. The lidar was located within 10 m of the shoreline which is aligned roughly north-south. A slightly curving shoreline places the beach $\sim$ 500 m west of the lidar at 3 km south of the lidar. It then curves to the east; placing the shore directly south of the lidar $\sim$ 3.5 km south of the lidar. The shore reaches a maximum distance east of the lidar, $\sim$ 350 m at $\sim$ 6 km south of the lidar. The bright structures in the image are wisps of steam-fog. The polygonal structures indicate an open cell convection pattern. Downward motion occurs in the clear central area of the cell producing convergence in the cell walls. This concentrates the steam-fog in the cell walls and produces sharply concentrated updrafts in the cell walls. On initial examination, these structures appear quite different than those previously observed in unstable surface layer flows (see Wilczack, 1984, for example). Since our initial LES model runs show evidence of similar structures, the model may help provide an explanation for the observed structure. This requires careful investigation.

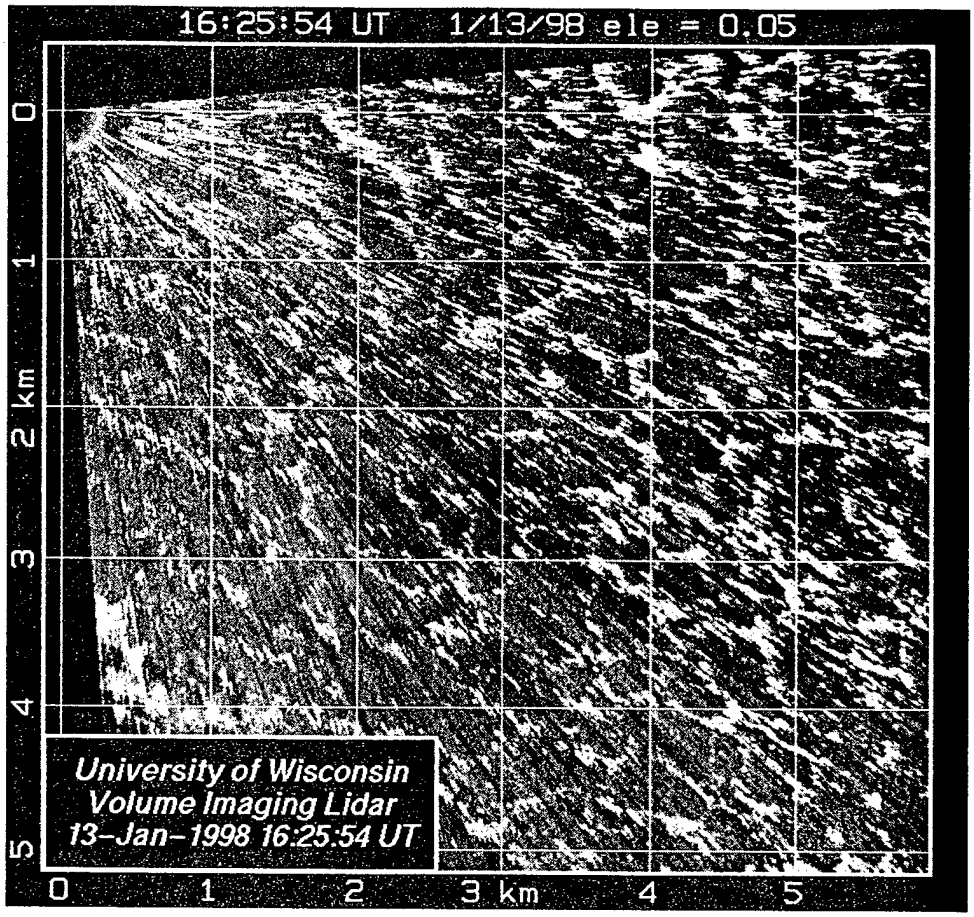

Figure 2. PPI of range-corrected backscatter intensity showing the organization of the steam-fog on 13 January 1998. The 10-minute average wind measured at the Coast Guard Station (located on the shoreline 3/4 km North of the lidar and 19.2 m above the surface) was 295° at 7.1 m/s. The air temperature was -20° C and the lake temperature was $\sim 6°$ C. The open-cells range in horizontal size from about 100 m at 1 km offshore to about 500 m at 5.9 km offshore.

Figure 3 shows the mean wind field observed in a 7 minute interval beginning at 10:24 UT on Jan 13, 1998. The data used to compute the winds consisted of 40 scans back and forth between azimuth angles of 70° and 176°. Laser shots were acquired at azimuth intervals of 0.08 degrees with the laser aimed horizontally at 5 m above the surface of Lake Michigan. A back and forth scan required ~ 24 seconds.

This wind field shows a region in the upper right hand corner with winds of ~ 9 m/s whereas most of the area has winds of ~ 7 m/s. Notice that the two regions are separated by a region of convergence. We suspect that this wind feature is related to the geometry of the shoreline; a prominent point extends into the lake a short distance north of the lidar location. There also appears to be an increase in the winds speed near the south end of the region. It is also possible that the ~ 7 m/s region in the center of the image represents a wind shadow caused by increased surface friction over the city of Sheboygan which lies

directly upwind of this area. At this point, these explanations are just speculations; it may be possible to add confidence to these explanations through computer models which include the shoreline topography.

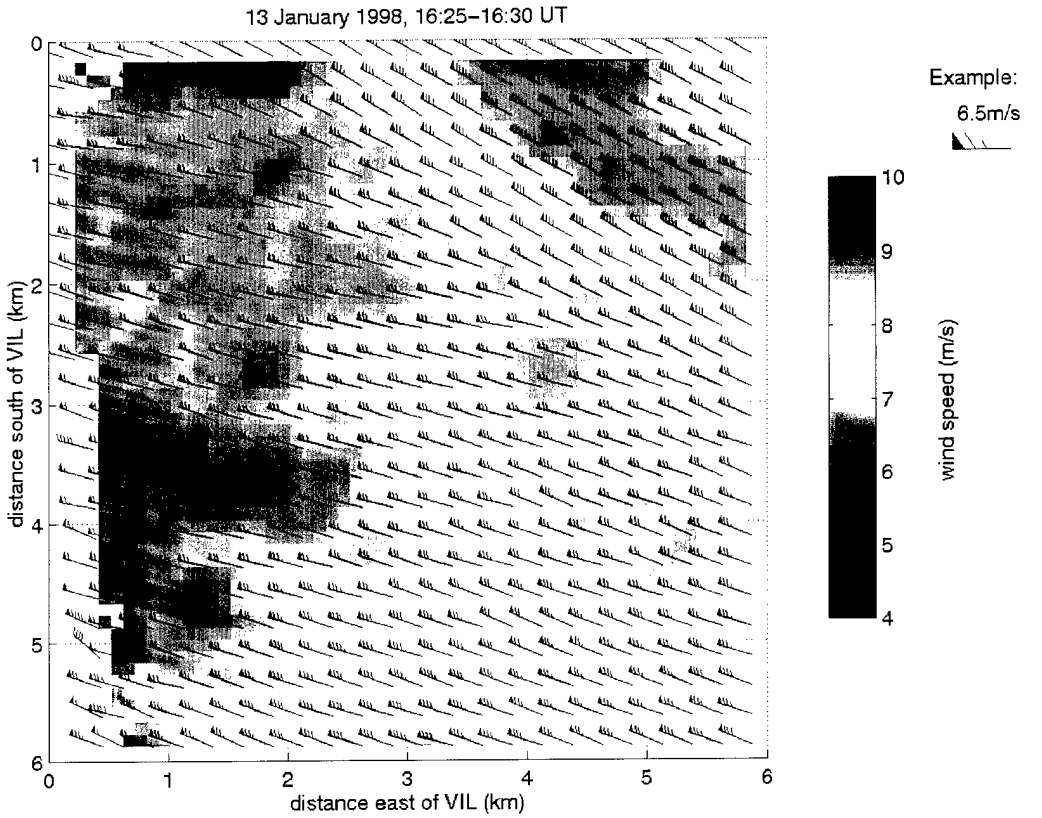

Figure 3. Wind vectors computed from 40 PPI scans acquired between 10:24:44 and 10:32:17 CST on January 13, 1998. The background color plot depicts the spatial variation of wind speed. Meteorological wind barbs are presented with single barbs indicating 1 m/s. Wind barbs are plotted at the centers of the first sub-area used in the correlation computation. At the edges of the scan where the sub-area are not completely covered by the lidar scan, the vectors are plotted at the center of gravity of the scanned area. Vectors are not plotted if less than 25% of the sub-area was covered by the lidar scan.

Figure 4 shows the divergence field computed from the wind vectors in figure 3. The divergence was computed as follows:

$$\nabla \cdot \vec{V}_{i,j} = \frac{u_{i+1,j} - u_{i-1,j}}{x_{i+1} - x_{i-1}} + \frac{v_{i,j+1} - v_{i,j-1}}{y_{j+1} - y_{j-1}}$$

where: $V_{i,j}$ is the velocity vector at point (x_i, y_j) with east-west and north-south components $u_{i,j}$ and $v_{i,j}$ respectively. Linear interpolation between grid points was used to provide a continuous color scale.

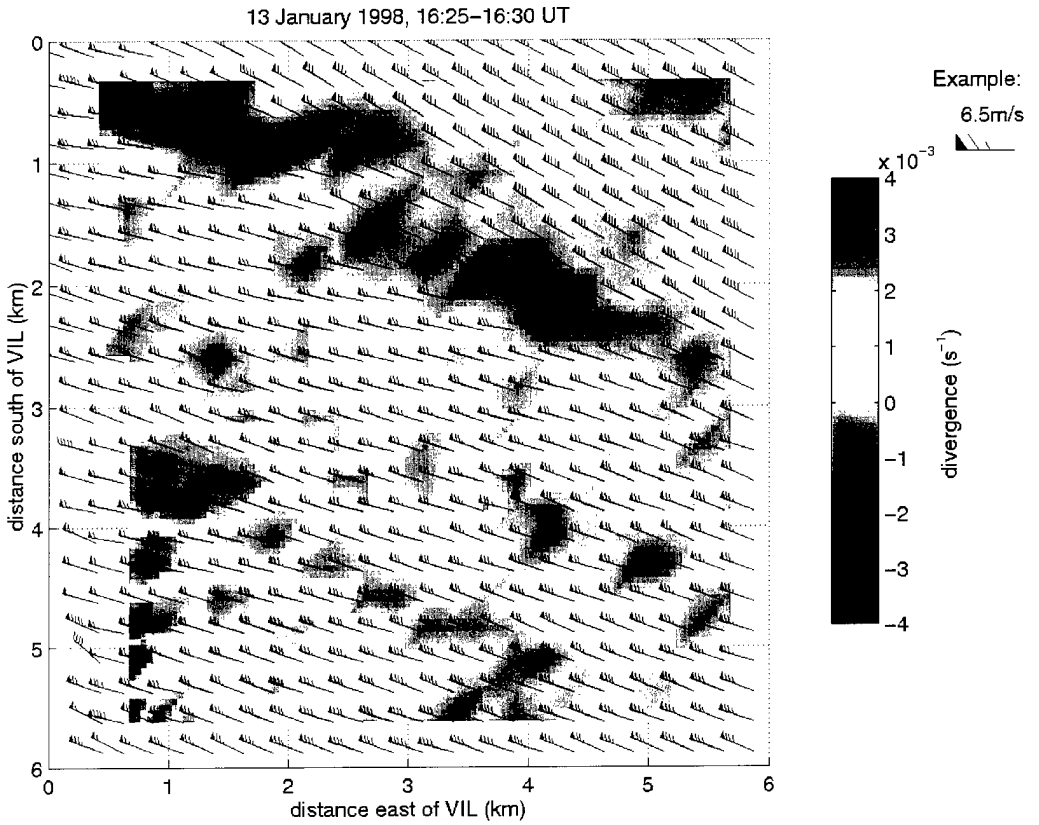

Figure 4. The divergence field computed from the velocity field presented in figure 3 is shown in colors. The wind vectors from figure 3 are superimposed.

Notice that the boundary between the faster moving air in the upper right-hand corner and the slower winds in the center is characterized by a convergence of $\sim 4 \cdot 10^{-3}$ s^{-1}. A somewhat weaker convergence line is present in the lower left of the picture and a hint of a third convergence line can be seen between the two more prominent lines. The divergence present in the far upper-right corner is consistent with the existence of an additional convergence band above the most prominent band. This set of parallel bands is consistent with the existence of longitudinal roll circulations. The spacing between these bands ranges from 1.0 to 1.8 km, yielding an average spacing of $\sim$ 1.5 km. Lidar images show that the boundary layer depth is $\sim$ 450 m at this time. Thus, if the bands are caused by longitudinal roll circulations, the ratio of roll spacing to roll depth is $\sim$ 3.3. Analytical models predict that this ratio should lie between 1 and 4, while radar observations provide values between 2 and 9 for roll convection on the downwind side of Lake Michigan during cold air outbreaks (Kelly, 1984).

Longitudinal rolls are routinely observed in the cumulus clouds which form over the lake during cold air outbreaks. This observation suggests that, under some conditions, the circulations may exist before the air encounters the lake. Furthermore, in this case, it seems likely that the circulation is triggered by an orographic feature. It is interesting to note that the spacing between the most prominent band and the adjacent bands, $\sim$ 1.8 km, is larger

than the spacing between the next two bands. This is consistent with the orographic forcing explanation of the prominent circulation, which makes it much more energetic and therefore larger than the surrounding circulations.

Figure 5 shows the vorticity field computed from the winds shown in figure 3. As expected the shear line in the upper-right of the picture corresponds to a band of enhanced vorticity. We would expect that this band, which combines strong convergence and strong vorticity, would promote the formation of steam devils. Steam devils were observed visually on this day. Unfortunately, we did not try to record the visual location of the steam devils. However,on some days we did note that they seemed to form preferentially in certain directions. We plan to inspect volume scans obtained near the time of this data to look for evidence of steam devils in the area of strong convergence and vorticity. The sign of the vorticity should determine the rotation direction the steam devils. It would be interesting to test this prediction in a future experiment.

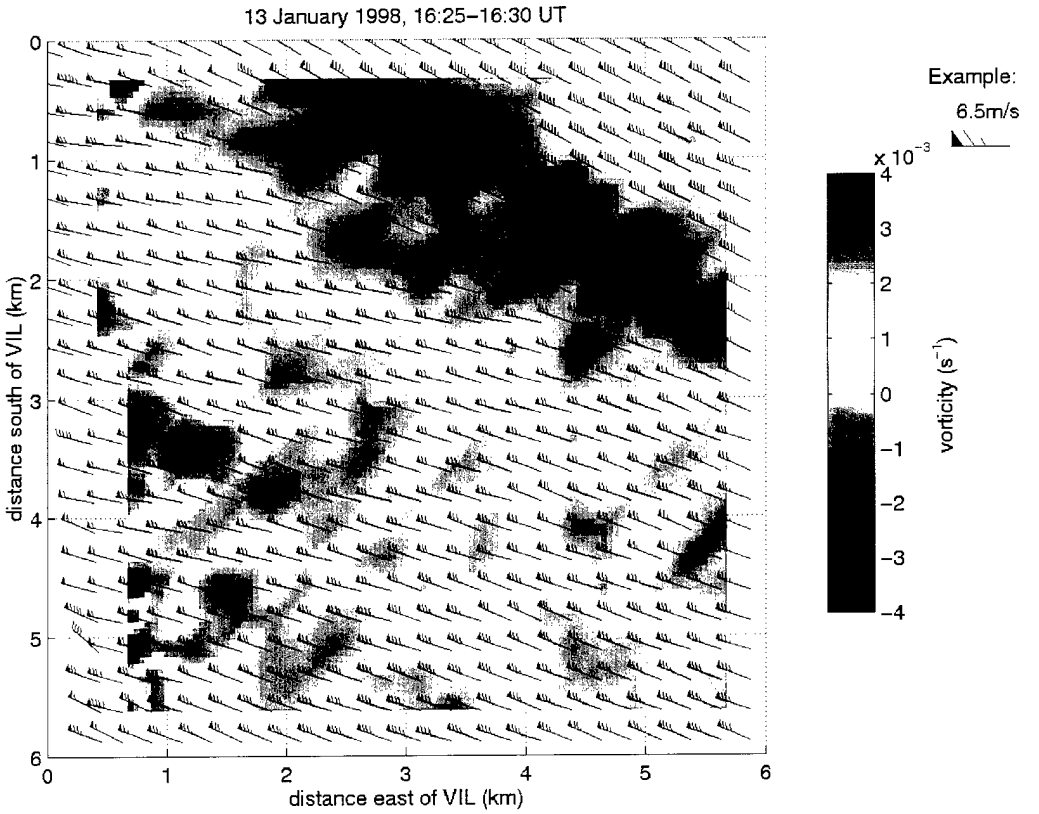

Figure 5. The vorticity field computed from the velocity field presented in figure 3 is shown in colors. The wind vectors from figure 3 are superimposed.

5.2 Data from January 10, 1998

Figure 6 shows steam fog structure at an altitude of 5 m observed in lidar scan obtained at 14:17 UT on January 10, 1998. The 19.2 m altitude wind at the Coast Guard station 3/4

km north of the lidar was from 236° at 6.3 m/sec and the air temperature was −16.7° C. Polygonal cells are once again visible in the steam fog.

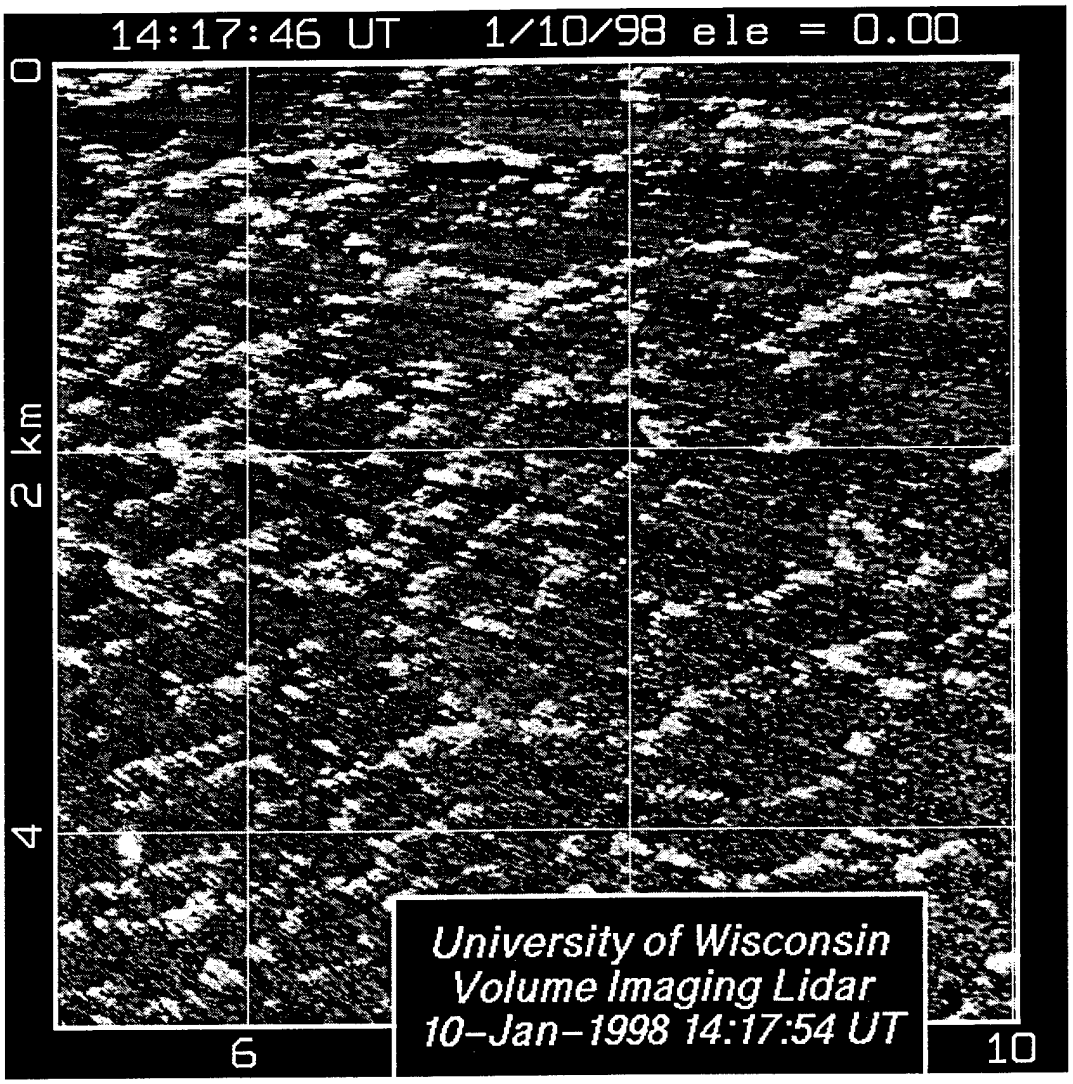

Figure 6. PPI of range-corrected backscatter intensity showing the organization of the steam-fog on 10 January 1998. The 10-minute average wind measured at the Coast Guard Station (located on the shoreline 3/4 km North of the lidar and 19.2 m above the surface) was 236° at 6.2 m/s.

Figure 7 shows the average wind field computed for data acquired between 14:16 and 14:57 UT. The wind shadow in the lee of the coastline is clearly visible. The wind shadow length varies with position. This probably reflects variations in the topography and surface roughness along the shore. The acceleration and veering of the wind as it leaves the shore is clearly seen in figure 8. This presents a north-south average of the wind speeds and directions along with a crude estimate of errors. The length of the error bars were computed from the variance of the values contributing to each north-south average. The plotted length of the

error bar is equal to the variance divided by the square root of the number of points ($\sqrt{24}$ in this case) contributing to the average. While these error bars provide an estimated upper bound for the random fluctuations in the wind, they are not true error estimates. They tend to underestimate the true error by failing to include systematic errors while at the same time tending to overestimate the errors because the true geophysical variability is included in the calculated variance.

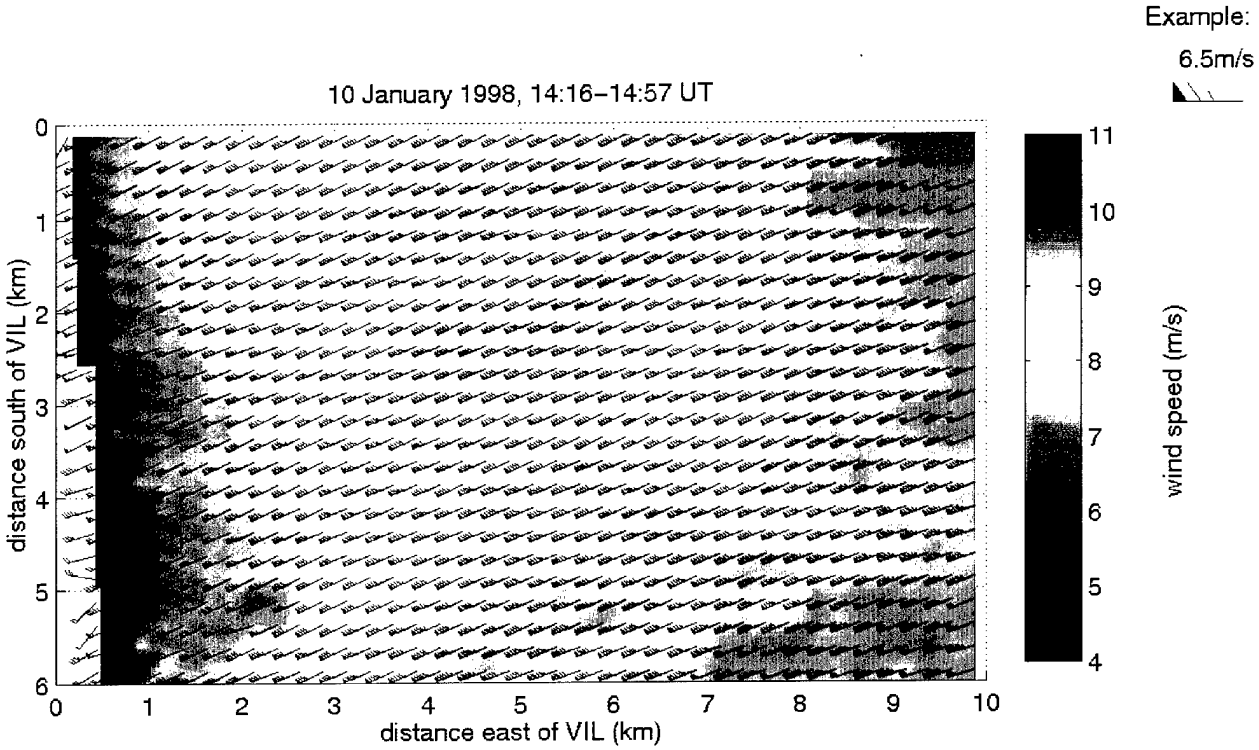

Figure 7. Wind vectors computed from 240 PPI scans acquired between and CST on January 10, 1998. Meteorological wind barbs are presented with single barbs indicating 1 m/s. Wind barbs are plotted at the centers of the first sub-area used in the correlation computation. At the edges of the scan where the sub-area are not completely covered by the lidar scan, the vectors are plotted at the center of gravity of the scanned area. Vectors are not plotted if less than 25% of the sub-area was covered by the lidar scan.

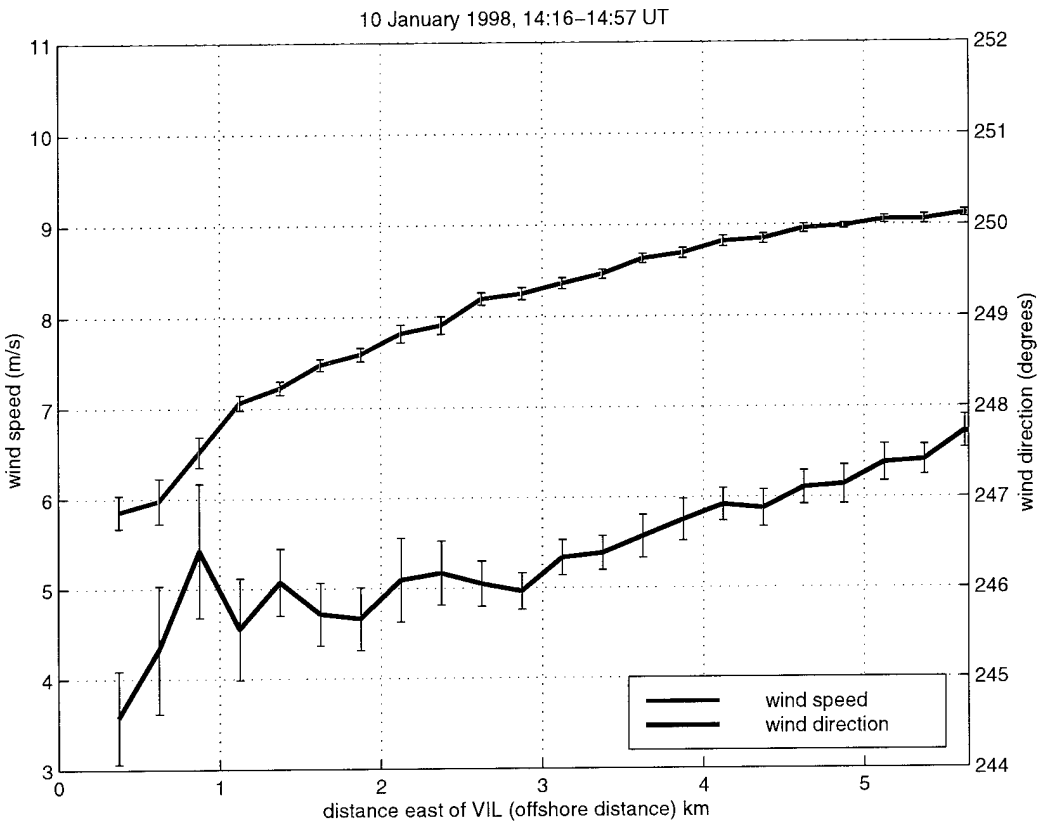

Figure 8. Average wind speed and direction as a function of distance from the shore between 14:15 and 14:57 UT on January 10, 1998. The acceleration and veering of the wind with offshore distance are clearly seen. This plot is computed from a north-south averaging of the data shown in figure 6. Only those vectors computed from areas completely covered by the lidar scan are used in the average.

Figure 9 shows the divergence field computed from the wind data in figure 7. Notice the strong divergence along the shoreline caused by the acceleration of the wind as it adjusts to the lower surface roughness lengths presented by the water relative to the land. A narrow band of divergence extends downwind from a point $\sim$ 3.2 km south of the lidar. The Edgewood power plant, which consists of a very large building complex, is located at this point on the shore and it appears as if this divergence feature may represent a building wake or possibly an artifact caused by the slow meandering of the weak surface aerosol plume emitted by the power plant. This is one of many intriguing observations which must be investigated carefully in our continuing data analysis.

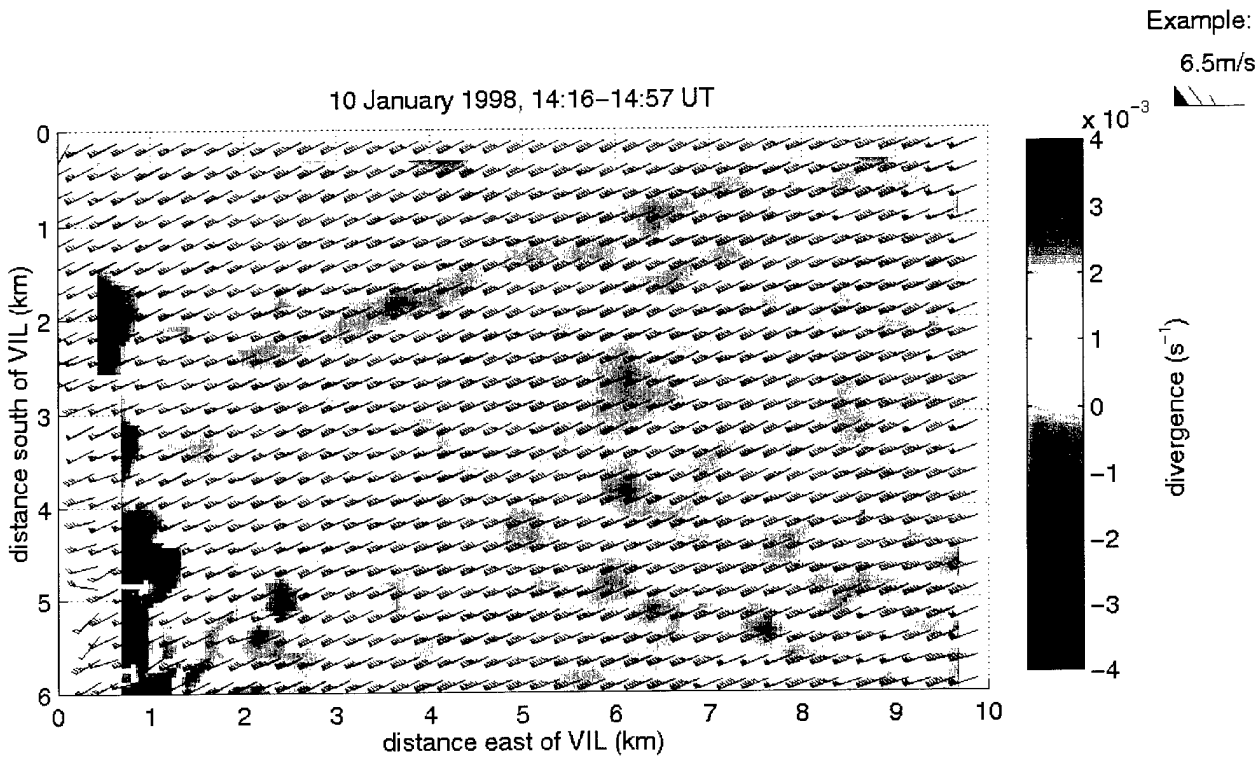

Figure 9. The divergence field computed from the velocity field presented in figure 7 is shown in colors. The wind vectors from figure 7 are superimposed.

Figure 10 presents the divergence as a function of distance from shore calculated from the data presented in figure 9. Random variations in the smoothed curve between 3.5 and 5.5 km from shore appear to be less than 10^{-4} s^{-1}. This is an encouraging result, since these results are expected to improve as the wind algorithms are optimized for this application.

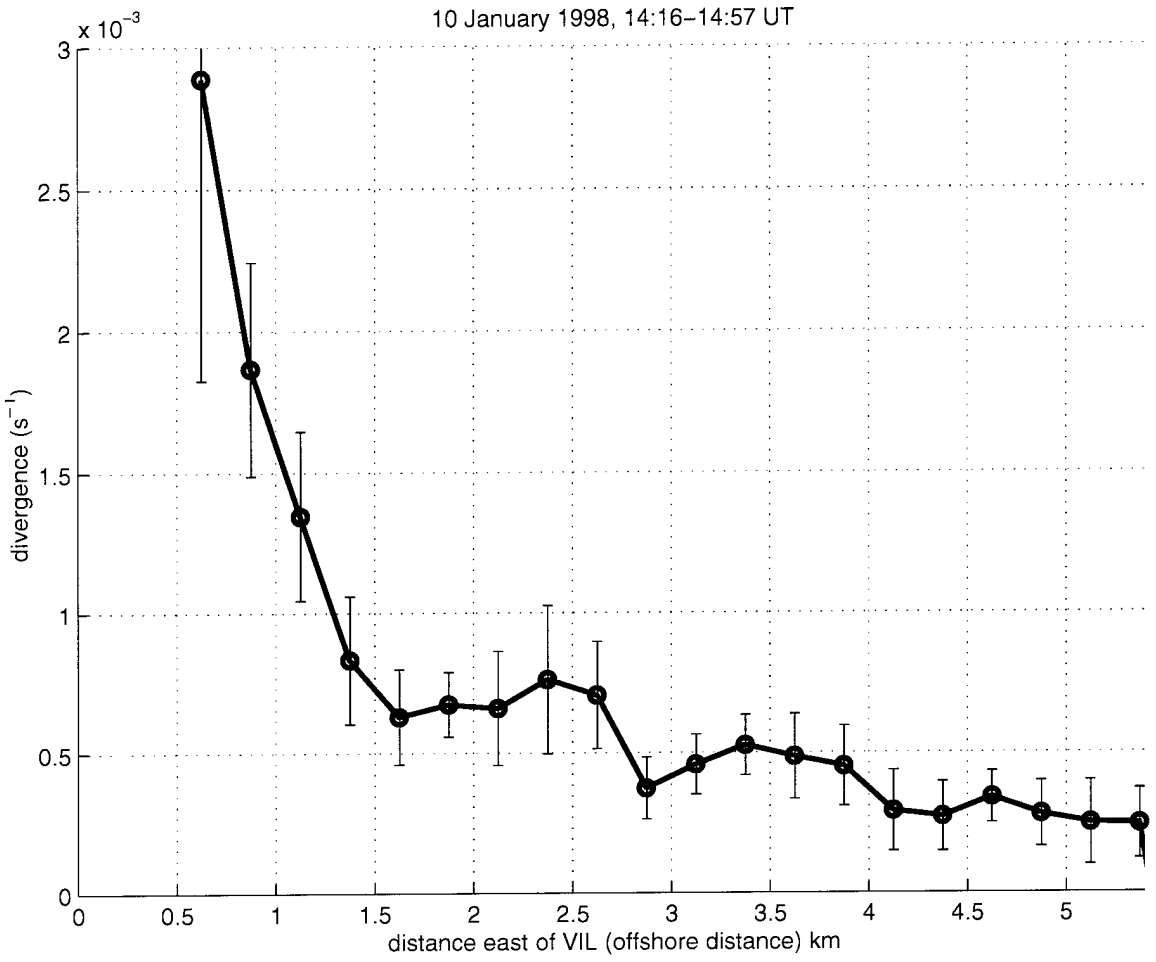

Figure 10. Divergence as a function of distance from the shore between 14:15 and 14:57 UT on January 10, 1998. The plotted points are the divergence values computed directly from the data presented in figure 9.

Figure 11 shows the vorticity field computed from the wind field shown in figure 7. Strong negative vorticity appears along the shoreline as the wind veers in response to the smaller friction over water. Here, the possible wake feature shown in the divergence field appears as a strong negative vorticity wake. At distances greater than $\sim$ 3 km from the shore there is evidence of a coupled band of positive vorticity north of the negative band.

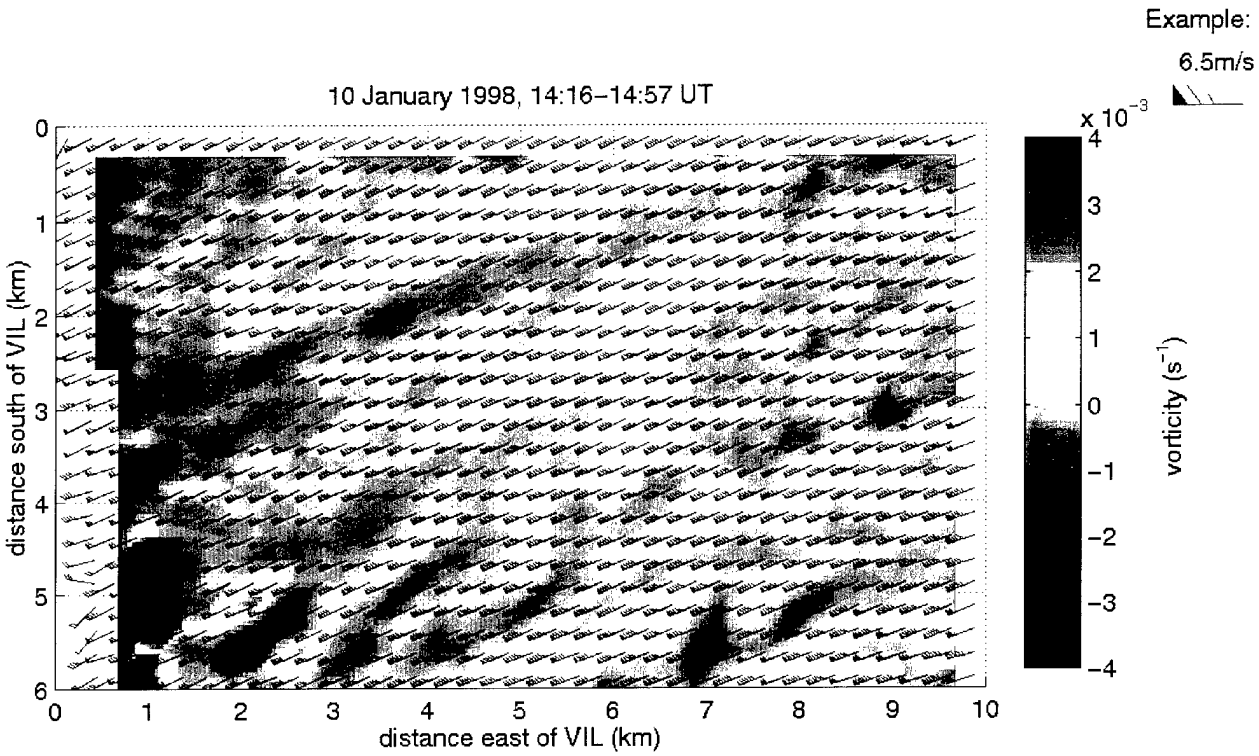

Figure 11. The vorticity field computed from the velocity field presented in figure 7 is shown in colors. The wind vectors from figure 7 are superimposed.

6 Preliminary LES modeling

The resolution of Large-Eddy-Simulations are typically limited by computer speed and memory capacity. Our computer resources have recently been improved with the support of the IBM corporation Shared University Research program. This IBM grant has provided us with an 8-processor model J50 computer with 2 Gb of memory and 50 Gb of disk.

Greg Tripoli has substantially restructured the University of Wisconsin Numerical Modeling System code to allow efficient operation on Symmetric Multi-Processor computers. We have taken this code, which was written for a Silicon Graphics computer, and modified it to run on our IBM system. Identical model runs have been performed on the SGI and IBM machines to confirm that that the model operation has not been affected by changing computers and operating systems.

Figure 12 shows sample output from a preliminary attempt to model the flow field at 14:00 UT on January 13, 1998. A domain 6 km in the east-west dimension, 3 km in the

north-south and 2.45 km in the vertical was considered. The model resolution was 15 m in the horizontal an contained 80 levels in the vertical. The vertical resolution near the ground was set to 1 m with geometrically increasing spacing up to 50 m at an altitude of 400 m. Above 400 m the vertical grid spacing was 50 m. This produces a grid domain of 400 by 200 by 80 with 6.8 million grid points. A time step of 0.25 second was used for the simulation. Figure 12 shows liquid water content and horizontal streamlines on the lowest model level, z= 1 m, after 16 minutes and 30 seconds of model time. The model utilized a fixed upwind (left edge of image) boundary condition derived from wind, temperature and humidity profiles measured with a National Center for Atmospheric Research CLASS radiosonde profile acquired at the Sheboygan airport ($\sim$ 10 km east of the lidar). An open boundary condition was used on the downwind boundary (right edge of image) and cyclical boundary conditions were used in the north-south direction. The surface temperature over Lake Michigan (6° C) was derived from NOAA satellite measurements while the land surface temperature was set equal to the air temperature ($-20°$ C).

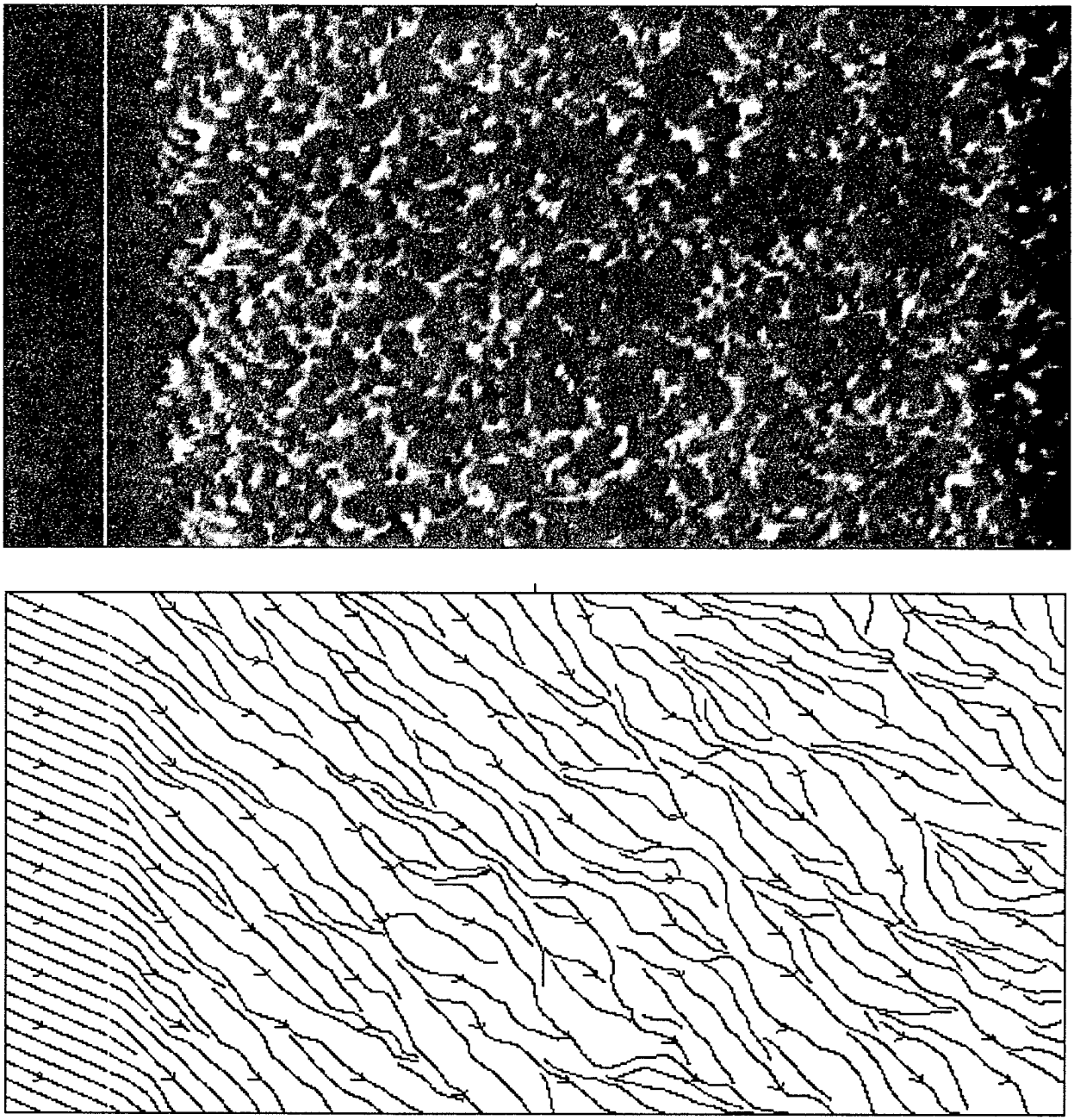

Figure 12. Steam fog computed by model at 1 meter above the surface after 16.5 minutes of simulation (upper panel) and streamlines for the same time (lower panel). The model domain is 6 km by 3 km and the shoreline is placed 600 m from the left edge of the domain (white line in upper panel).

It is encouraging to note that this preliminary model run shows open cell convection patterns in the steamfog which are similar to those shown by the lidar. Earlier model runs

at (see attached conference abstracts) showed the development of longitudinal roll structures near the shore with a cross wind wavelength dependent on model resolution. Although the current 15 m grid seems to have nearly eliminated these features, the effects of model resolution must be investigated further. Model runs with a fixed 15 m vertical and horizontal resolution do not generate steam fog. This has forced the use of grids with vertical spacings which are much smaller than the horizontal spacings. The impact of these asymmetric grids on model performance must be investigated.

A major goal of our future work involves quantitative comparisons between the model output and the lidar observations. These comparisons will involve wind, divergence and vorticity fields along with their variations with offshore distance. Lidar volume scans will be analyzed to provide vertical profiles which can be compared to the model. Additional comparisons are planned between eddy lifetimes and eddy dimensions, alignments and aspect ratios.

7 References

- Kelly, R. D., 1984: Horizontal Roll and Boundary-Layer Interrelationships Observed over Lake Michigan, *J. of Atmospheric Sciences*, **41**, 1816-1826.
- Schols, J. L., and E. W. Eloranta, 1992: The calculation of area-averaged vertical profiles of the horizontal wind velocity from volume imaging lidar dat ., *J. of Geophysical Research*, **97**, 18395-18407.
- Wilczak, J. M., 1984: Large scale eddies in the unstable atmospheric surface layer., *J. of Atmospheric Sciences*, **41**, 3537-3550.
- Piironen, A. and E. W. Eloranta, 1995: An accuracy analysis of the wind profiles calculated from Volume Imaging Lidar data, *J. of Geophys. Res.*, **100**, 25559-25567.
- Young, P. and E. W. Eloranta, 1995: Calculation of divergence and vertical motion from volume-imaging lidar data, *J. of Geophys. Res.*, **100**, 25577-25583.

8 Degrees based on ARO supported work

- Gurer, K, 1995: 3-D comparisons of simulated large eddy structures with lidar observations. *Ph.D. Thesis, University of Wisconsin-Madison*, 159 pp.
- Piironen, A. K.,1994: Analysis of Volume Imaging Lidar Signals. *Ph.D. Thesis, University of Joensuu, Joensuu, Finland*, 77 pp.

9 Personnel supported

The following personnel received support under this ARO grant.

Edwin Eloranta	Senior Scientist
Dan Forrest	Computer Programer
Patrick Ponsardin	Optical Engineer
Jim Hedrick	Mechanical Engineer
Antti Pirronen	Researcher
Ralph Kuehn	Graduate Student
Shane Mayor	Graduate Student

10 Journal Papers

The following Journal papers report on work supported on previous ARO grants. However the publication did not occur until well after the end of those grants, thus these papers are included with the current report. Work on publications describing lake-ICE research is just beginning.

- Avissar, R., E. W. Eloranta, K. Gurer and G. J. Tripoli, 1998: An evaluation of the large-eddy simulation option of the regional atmospheric modeling system in simulating a convective boundary layer: a FIFE case study. *J. of Atmospheric Sciences*, **55**, 1109-1130.

- Pirronen, A., K. and E. W. Eloranta, 1995: Accuracy analysis of wind profiles calculated from volume imaging lidar data, *J. of Geophysical Research*, **100**, 25559-25567.

- Pirronen, A., K. and E. W. Eloranta, 1995: Convective Boundary layer mean depths and cloud geometrical properties obtained from volume imaging lidar data. *J. of Geophysical Research*, **100**, 25569-25576.

- Young, P. W. and E. W. Eloranta, 1995: Calculation of divergence and vertical motion from volume imaging lidar data, *J. of Geophysical Research*, **100**, 25577-25583.

11 Conference Presentations

Research results obtained under this grant have been reported in a series papers delivered at scientific conferences. The titles of the papers are listed below and abstracts are appended to this report.

- **Extracting quantitative information on Convective boundary layers from aerosol lidar data.** Edwin W. Eloranta, American Meteorological Society 12th Symposium on Boundary Layers and Turbulence Vancouver, BC July 28, Aug 1 1997

- **Near-Shore Boundary Layer Structure over Lake Michigan in Winter.** Edwin W. Eloranta, Ralph E. Kuehn, Shane D. Mayor and Patrick, American Meteorological Society 13th Symposium on Boundary Layers and Turbulence Dallas, TX, January, 1999.

- **Comparison of microscale convection patterns seen in lidar data and large-eddy simulations** Shane D. Mayor, Gregory J. Tripoli, Edwin W. Eloranta, and Bradley D. Hoggatt, 13th Symposium on Boundary Layers and Turbulence Dallas, TX, January 1999.

- **Summary of Volume Imaging Lidar (VIL) Preliminary Results from the Lake-Induced Convection Experiment (Lake-ICE)** Shane D. Mayor, Edwin W. Eloranta, Ralph Kuehn, and Patrick Ponsardin, 19th-International Laser Radar Conference, Annapolis, MD, July 6-10, **This paper was selected as the best poster paper of the conference.**

- **Lidar Observations of a Land-Breeze Circulation**, E. W. Eloranta, R. Kuehn and S. Mayor, 19th-International Laser Radar Conference, Annapolis, MD, July 6-10, 1998

- **Volume Imaging Lidar Observations of Atmospheric Boundary Layer Structure over the western edge of Lake Michigan**, Ed Eloranta, Shane Mayor, Ralph Kuehn, Patrick Ponsardin, and Jim Hedrick, 4th International Symposium on Tropospheric Profiling, Snowmass, CO, Sept 20-25, 1998.

American Meteorological Society
12th Symposium on Boundary Layers and Turbulence
Vancover, BC July 28 - Aug 1, 1997

EXTRACTING QUANTITATIVE INFORMATION ON CONVECTIVE BOUNDARY LAYERS FROM AEROSOL LIDAR DATA

E. W. Eloranta
University of Wisconsin, Madison, Wisconsin

Introduction

Quantitative evaluation of Large Eddy Simulations (LES) of the convective boundary layer are hampered by statistical sampling errors in measurements and lack of knowledge of the mesoscale divergence. Measurements obtained from towers and remote sensors pointing in fixed directions can only sample those convective cells which drift overhead. Since LES modeling of convective boundary layers is most easily accomplished for light wind conditions, these fixed sensors sample very few plumes and the statistics derived are hopelessly inadequate to describe rapidly evolving boundary layers. Aircraft mounted instruments penetrate a larger number of cells, but still have difficulty generating stable statistical estimates within the 10 km domain of a typical LES. Furthermore, the time required to execute flight legs at several altitudes makes it difficult to generate accurate vertical profiles in rapidly evolving convective boundary layers.

LES evaluation would be greatly improved if the entire 3-dimensional model domain could be observed with a spatial and temporal resolution equivalent to the model resolution. Remote sensors which actively probe the 3-d volume can provide the needed information.

Rapidly scanning lidars, such as the University of Wisconsin Volume Imaging Lidar (VIL) provide vivid images of convective boundary layer structure with the required spatial and temporal resolution over typical LES model domain sizes (Fig. 1). In a typical 3-min scan the VIL provides $\sim$ 20 million measurements of aerosol backscattering in a 3-dimensional volume above a $\sim$ 100 km^2 surface area. The challenge lies in deriving quantitative information from the aerosol backscatter data which can be compared to the LES.

This paper will describe how time-resolved 3-D aerosol backscatter measurements can be processed to yield: 1) vertical profiles of wind speed and direction, 2) convective eddy shapes and orientations, 3) correlation decay times for the convective field, and 4) the mesoscale divergence. In addition, the lidar easily generates horizontal maps of boundary layer depth, cloud base altitudes and cloud coverage.

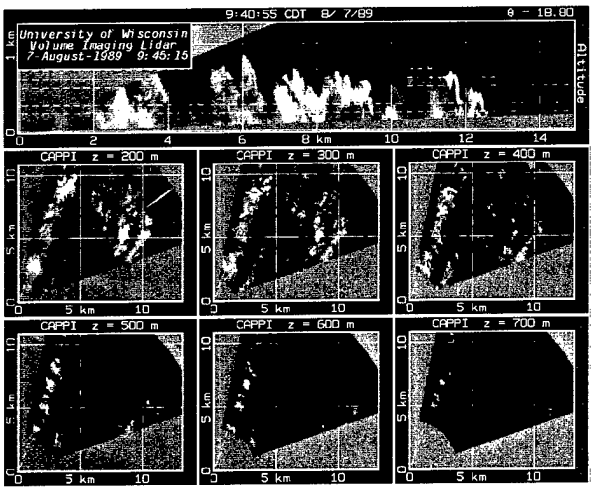

Figure 1. Lidar Images of clear air convective structure. The upper panel shows a range-height cross section and the lower 6 panels show horizontal cross sections. Bright areas indicate stronger lidar returns and therefore greater aerosol scattering.

The boundary depth as a function of time is easily determined from the horizontal variance of the aerosol backscattering. This variance exhibits a maximum at the top of the boundary layer where mixed layer air alternates with clear air from above.

Motions of the lidar observed aerosol structure can be used to derive wind speed and direction profiles. Winds are derived by computing two-dimensional cross correlations between successive VIL images of aerosol structure on horizontal planes. Because these measurements are averaged over the $\sim$ 100 km^2 lidar scan area, it is possible to obtain stable estimates of the wind even in the presence of strong turbulent fluctuations (Fig. 2).

Horizontal divergence can also be measured from images of aerosol structure on horizontal planes. While determining the mean wind, the cross-correlation between successive images is computed after applying linear stretches and compressions to the horizontal distances in one of the images. The stretch or compression scaling producing the highest correlation is then used to compute the divergence.

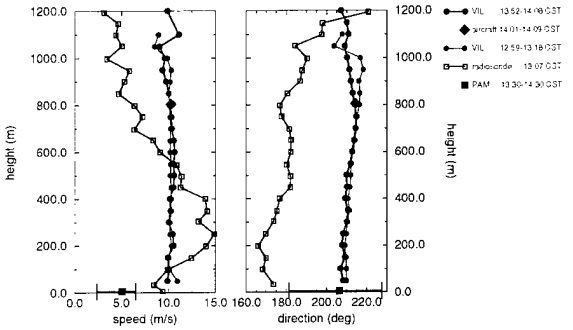

Figure 2. Wind Profiles observed with the VIL and with an optically tracked radiosonde balloon on July 29, 1989 (Piironen and Eloranta, 1996). Included are 15 km flight leg averaged winds measured from an aircraft and measurements from a 10 m tower. The 10 m winds are 1 hour averages, averaged over 8 locations near the lidar.

Two-dimensional autocorrelation functions computed from images of the aerosol backscatter along a horizontal plane provide information on the size, shape, and orientation of convective plumes. Figure 3 shows the elongation and orientation of plumes with respect to the mean boundary layer wind and the wind shear across the boundary layer.

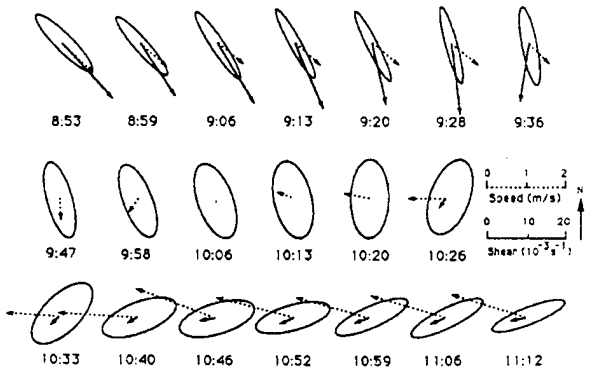

Figure 3. Plume Geometry The orientation and horizontal ellipticity of convective cell relative to the mean wind and vertical shear vectors observed on June 7 ,1983 are plotted as a function of time (Ferrare and Eloranta 1991). The convective layer mean wind and the shear across the layer are also shown. Note that the ellipticity is strongly correlated with the wind speed while the orientation is correlated with the shear vector.

The cross-correlation function can also be computed as a function of the time separation between images (Fig. 5). This gives information on the spatial scale of plumes and the decay rate of structure which can be directly compared with LES model results.

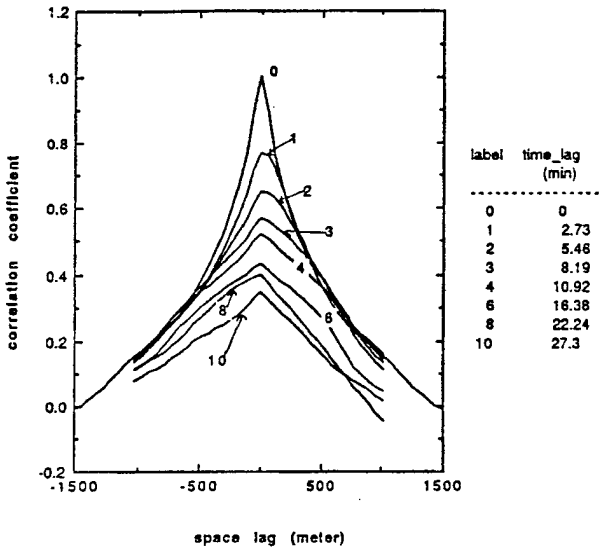

Figure 5. Spatial correlation functions as a function of time delay between lidar images measured with the Volume Imaging Lidar in the convective boundary layer (Sun, 1989). Correlations have been aligned with maximum at zero lag to remove mean wind displacement.

Acknowledgments

This research was supported by Army Research Office Grant DAAH04-94-G-0022.

References

Sun, C., 1989: 3-D spatial and temporal correlation functions of aerosol structures in the convective boundary layer, *University of Wisconsin-Madison Masters Thesis,* 97 pp.

Ferrare, R.A., J.L. Schols, E.W. Eloranta, and R. Coulter, 1991: Lidar Observations of Linear Convection During BLX 83, *J. of Appl. Meteor.*, **30**, 312-326.

Piironen, A. and E. W. Eloranta, 1995: Convective boundary layer mean depths, cloud base altitudes, cloud top altitudes, cloud coverages, and cloud

shadows obtained from Volume Imaging Lidar data. *J. of Geophys. Res.*, **100**, 25569-25576.

Piironen, A. and E. W. Eloranta, 1995: An accuracy analysis of the wind profiles calculated from Volume Imaging Lidar data, *J. of Geophys. Res.*, **100**, 25559-25567.

Young, P. and E. W. Eloranta, 1995: Calculation of divergence and vertical motion from volume-imaging lidar data, *J. of Geophys. Res.*, **100**, 25577-25583.

Gurer, K, 1995: 3-D comparisons of simulated large eddy structures with lidar observations. *Ph.D. Thesis, University of Wisconsin-Madison*, 159 pp.

American Meteorological Society
13th Symposium on Boundary Layers and Turbulence
Dallas, TX, January 1999

Near-Shore Boundary Layer Structure over Lake Michigan in Winter

Edwin W. Eloranta, Ralph E. Kuehn, Shane D. Mayor and Patrick Ponsardin
University of Wisconsin-Madison
1225 W. Dayton St., Madison, Wisconsin, 53706, USA
phone: 608-262-7327, fax: 608-262-5974, e-mail: eloranta@lidar.ssec.wisc edu

Introduction

The wintertime flow of cold air over warm water produces a vigorous growing convective boundary layer along the upwind shore of Lake Michigan. This boundary layer, which increases in depth with distance from the upwind shore, provides an attractive setting in which to observe the development of convective structures. The water surface provides a lower boundary with nearly uniform temperature and flat topography to facilitate model calculations.

Figure 1. The lidar was located on the West shore of Lake Michigan at Sheybogan.

This paper presents observations gathered by the University of Wisconsin Volume Imaging Lidar (VIL). The lidar was deployed on the lake shore at Sheboygan, WI, as part of the Lake Induced Convection Experiment (Lake-ICE). The lidar observations were designed to provide data to test Large Eddy Simulation models. Data were acquired on 9 days between December 5, 1997 and Jan 22, 1998. Supplementary local data were collected by an NCAR integrated sounding system (ISS) located 10-km west of the lidar and by the National Data Buoy Center's SGNW3 weather station located 3/4-km north of the lidar.

Convective structures

A variety of convective structures were observed during periods when cold air advected over the warm water. Of particular interest are images showing open cells with downward motion in the center, upward motion in narrow cell walls, and approximately hexagonal cross sections. These were observed on both January 10th and 13th. An image of these cells observed on Jan 10th is shown in figure 2.

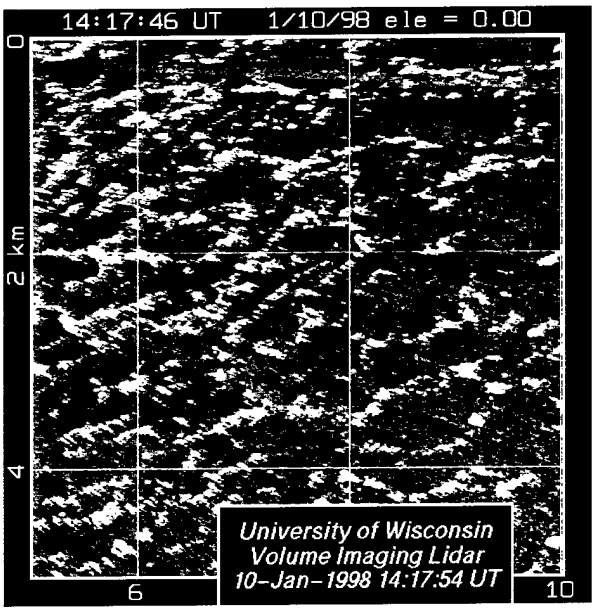

Figure 2. Enlargement of a 25-km^2 region 5-10 km offshore from a PPI image of range-corrected backscatter intensity. The image shows open-cell organization of convection in the steam-fog over the lake during a cold air outbreak on 10 January 1998. Note the approximately hexagonal shape of the cells. At the shore, the mean wind during this time was from 236° at 6.5 m s^{-1} and the air temperature was -16.7° C.

Lidar volume scans obtained on January 13 showed narrow columns of steam-fog rising nearly to the the top of the mixed layer at $\sim$ 400 meters. Steam-devils were observed visually during this period. Large eddy simulations of the flow field for this day are presented in a separate paper (Mayor et al.) at this conference.

Closed cells with upward vertical motion in the center were observed on January 19. Figure 3 shows a azimuthal scan obtained at an elevation angle of 1.5°. Bright echos are seen at a range of $\sim$ 9 km where the lidar beam hits the bottoms of clouds at at an altitude of $\sim$ 250 m. At 16 UTC the Coast Guard station reported a temperature of -4.1° C with a wind of 2 m/s from a direction of 300°.

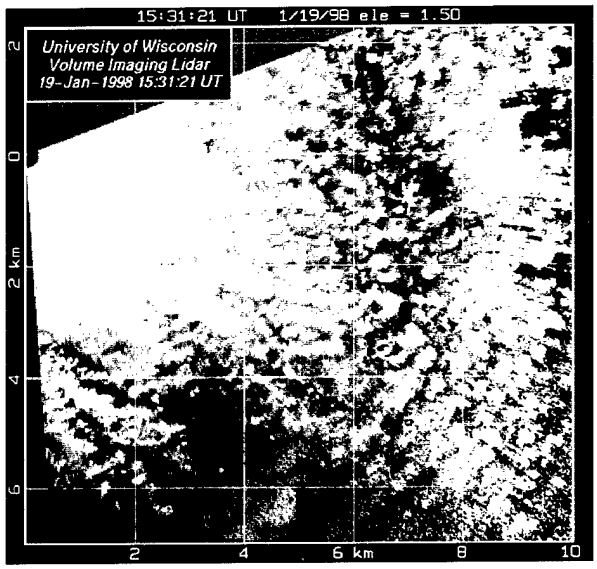

Figure 3. Closed cell convection observed at 15:01 UTC on January 19, 1998. An area of 10 by 9 km is shown. The lake shore is located approximately along the left edge of the the image. At the lidar the beam is $\sim$ 5 m above the lake surface. The 1.5° elevation angle increases the altitude to 255 m at a range of 9 km.

Land-breeze front

Vivid images of a land-breeze front and its temporal evolution were recorded on December 21, 1997. A large high-pressure system centered northeast of Lake Huron moved slowly eastward during the observation period. The resulting pressure gradient supported a weak southeasterly (on shore) synoptic flow. Figure 4 shows the wind speed and direction measured at the Coast Guard station.

The morning low temperature at the Sheboygan airport ($\sim$ 10 km inland from the lidar) was -6° C and it occurred at 14:00 UTC. The airport temperature rose slowly to -1° C by 17:00 UTC. The morning low temperature at the Sheboygan Coast Guard station (3/4 km north of the lidar on the shore

line) was −3.4° C at 11 UTC and the temperature rose to 1.6° C at 18 UTC. NOAA-satellite derived temperatures for the water offshore from the lidar were between 4° and 5° C.

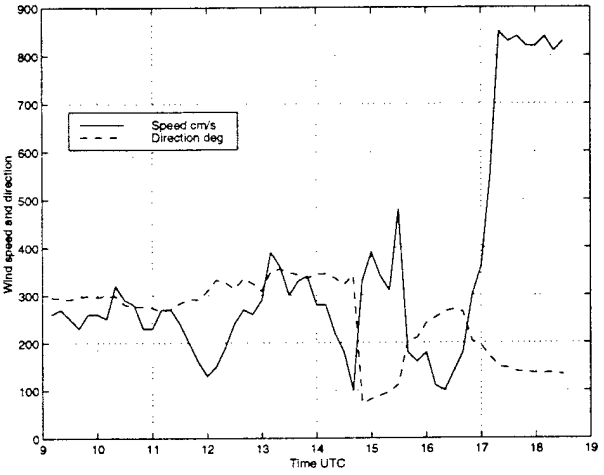

Figure 4. Wind speed and direction measured at the Sheboygan Coast Guard station between 9:00 and 18:30 UTC. The Coast Guard station is located 3/4-km North of the lidar site. Notice that the land-breeze front breaks down at 17:00 UTC under the influence of a weakening land-water temperature differential.

The lidar recorded volume scans between 13:12 UTC and 15:21 UTC. Each volume scan provided 101 separate RHI scans (0−15° elevation) in the azimuth range between 126° and 176°. The volume scan was repeated at intervals of 187 seconds. Figure 5 shows a sample image derived from one of these scans. This image includes one RHI scan along with two constant-altitude cross section created from the same volume scan. Due to the small format available in these proceedings, the horizontal cross sections are enlarged to show only a small portion of the 12-km north-south extent of the lidar images.

The RHI image shows that the front decreases in depth with distance from the shore. It also shows the thin bright land-breeze outflow layer within ∼ 20 m of the surface; this is the cold layer of air sliding out over the water against the synoptic flow. Animation of the RHI cross section shows that the land-breeze outflow is confined to a thin layer near the surface. This air appears to flow along the surface to the front where it rises in a strong convergence zone and is then swept back inland in the layer above the outflow. This return flow appears to undergo strong mixing with the marine boundary layer as it is forced up over the land-breeze front. This mixing is evident in the decreased brightness of the upper part of the front near the shore. This decrease of brightness can also be seen in the 110-m cross section which is brightest at the outer edge for the front where air from the surface outflow is being lofted in the convergence zone. Animations show the presence of gravity-wave crests running parallel to the shoreline in the upper part of the front. Point-target-echos also indicate the presence of sea gulls soaring in the air lifted over the front.

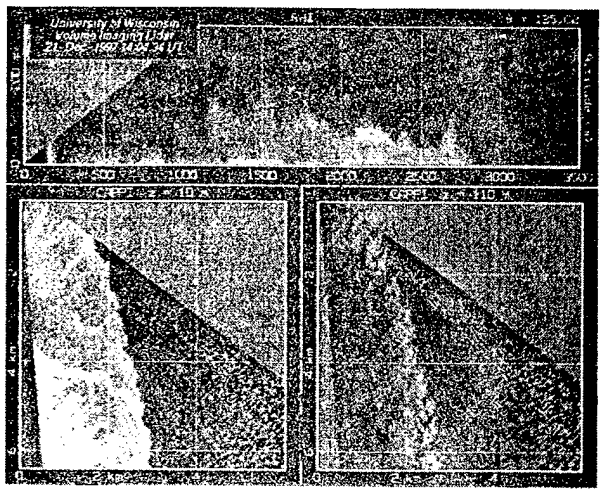

Figure 5. The land-breeze front observed at 14:04 UTC on December 21, 1997. The top panel shows a RHI cross section extending from the surface to an altitude of 300 m and a maximum horizontal range of 3500 m. The RHI is oriented at a compass heading of 134 degrees. The bottom panels show horizontal cross sections over a 6- by 6-km square area at altitudes of 10 m (left) and 110 m (right). North is at the top of the horizontal cross sections and the shoreline runs roughly along the left edge of the images.

The 10-m constant altitude scan shows the cold aerosol laden offshore flow in the land-breeze as an aerosol laden region which is roughly parallel to the shoreline of the lake. When a sequence of the 10-m altitude cross sections are animated, motions of the aerosol structures inside the lake-breeze front show a westerly flow. With careful enhancement of this cross section we can also see aerosol inhomogeneities beyond the front moving in a easterly flow.

Between 15:24 and 16:46 UTC the lidar was aligned horizontally and scanned back-and-forth to produce PPI scans between an azimuth of 85° and 176°. These were acquired with an angular separation between profiles of 0.08° providing a scan time of 12 seconds. Animations of these scans show the position of the land breeze fluctuating in a series of surges and regressions. The outflow wind is made clearly evident by the motion of aerosol inhomogeneities. The signal strength was sufficient to provide usable images of the front out to $\sim$ 12 km south of the lidar. Visual observations during this period showed the lake to be calm without capillary waves near the shore. Offshore, at a distance which appeared consistent with the lidar imaged front, the water surface turned dark and disturbed by the on shore flow. Figure 6 presents wind speed and direction as a function of distance from shore. These measurements were obtained from the motion of aerosol inhomogeneities using algorithms presented by Pirronen and Eloranta, 1995; and Schols and Eloranta 1992. These winds are averaged over a period of 47 minutes and a north-south band extending from from 1 to 2 km south of the lidar. The measurements were taken $\sim$ 5 m above the lake surface.

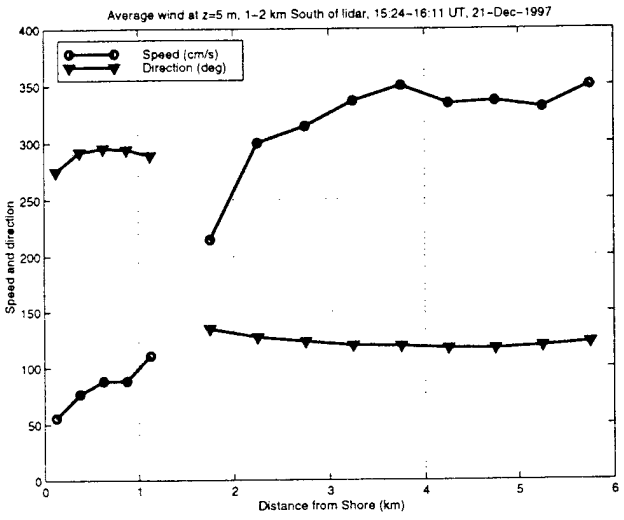

Figure 6. Wind speed and direction as a function of the distance from shore at 5 m above the lake surface. During the 47 min averaging period the front position oscillated slightly in the east-west direction. Winds are only plotted for positions which were always on the same side of the front. This produces a gap in the measurements at ~ 1.5 km from shore.

Acknowledgments

This work was made possible by NSF grant number ATM9707165 and ARO grant number ARO DAAH-04-94-G-0195.

References

- Pirronen, A., K. and E. W. Eloranta, 1995: Accuracy analysis of wind profiles calculated from volume imaging lidar data, *J. of Geophysical Research*, **100**, 25559-25567.

- Schols, J. L., and E. W. Eloranta, 1992: The calculation of area-averaged vertical profiles of the horizontal wind velocity from volume imaging lidar dat ., *J. of Geophysical Research*, **97**, 18395-18407.

American Meteorological Society
13th Symposium on Boundary Layers and Turbulence
Dallas, TX, January 1999

Comparison of microscale convection patterns seen in lidar data and large-eddy simulations

Shane D. Mayor, Gregory J. Tripoli, Edwin W. Eloranta, and Bradley D. Hoggatt
Department of Atmospheric and Oceanic Sciences, University of Wisconsin
1225 W. Dayton St., Madison, Wisconsin, 53706, USA
phone: 608-263-6847, fax: 608-262-5974, e-mail: shane@lidar.ssec.wisc.ed u

Introduction

Large eddy simulations (LESs) provide an attractive way of developing parameterizations for large-scale models such as global climate and weather forecast models. This is because they provide 4-D information which can potentially be used to compute fluxes with sampling errors that are much smaller than those made from in situ measurements. LESs, however, are only viable if we have confidence in their solutions. In particular, high resolution 4-D measurements are needed to test the LESs ability to accurately simulate the organization of convection such as linear and cellular boundary layer circulations. The objective of our research is to demonstrate the usefulness of volume imaging lidar data in LES validation.

To do this, we deployed the University of Wisconsin Volume Imaging Lidar (UW-VIL) at a site on the western edge of Lake Michigan and observed the growth of the convective boundary layer (CBL) over the water during cold-air outbreaks. We also ran the University of Wisconsin nonhydrostatic modeling system (UW-NMS) with microscale grid spacing to simulate lake-induced CBLs. This nonhomogeneous environment offers the advantages of a wide range of CBL depths and convective organization patterns within a simulation domain and requires substantially less computer time when compared to homogeneous CBL simulations that must be run for a large part of the diurnal cycle before several large-eddy turn-overs are obtained.

Previous work using VIL data to validate LES can be found in Avissar *et al.* 1998.

Observations

The UW-VIL was deployed in Sheboygan, Wisconsin, for the Lake-Induced Convection Experiment (Lake-ICE) during December of 1997 and January of 1998. The site (43°44′N, 87°42′W, 176 m ASL) was located within 10 m of the western shore of Lake Michigan. The VIL's beam-steering-unit (the point at which lidar beam is transmitted from) was located approximately 5 m above the lake surface. Thus, horizontal scans (PPIs) at 0° elevation allowed us to map the horizontal distribution of aerosol and steam-fog in a plane approximately 5 m above and parallel to the surface of the lake. Figure 1 is a PPI scan of this type. Steam-fog and hygroscopic aerosol produced a high-scattering tracer near the lake surface.

In addition to measuring aerosol scattering on horizontal slices through the surface layer, the VIL is capable of making vertical slices (RHIs) through the entire mixed layer and mapping the 3-D structure of aerosol scattering in the boundary layer. By rapidly moving the laser beam in a series of RHIs,

each with a slightly increased azimuth angle, we can measure the 3-D structure. For example, a volume scan spanning 40° in azimuth and 15° in elevation angle requires about 2 minutes. A typical change in elevation angle between two laser pulses during an RHI is 0.23°. By repeating such volume scans, we can also monitor the temporal evolution of the structures.

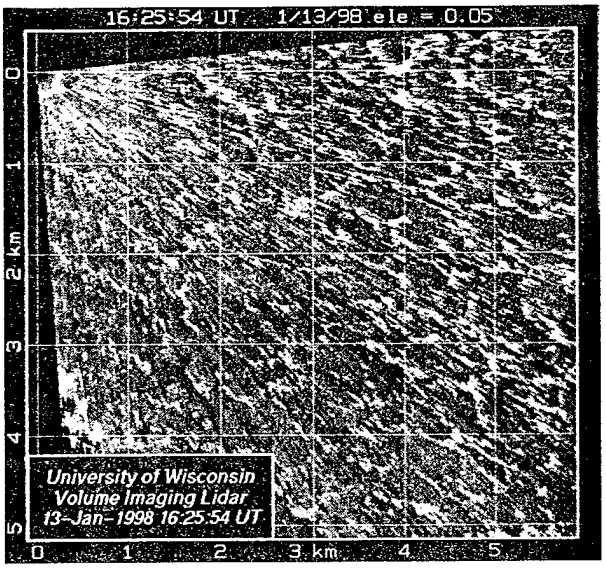

Figure 1. PPI of range-corrected backscatter intensity showing the organization of the steam-fog on 13 January 1998 from a few hundred meters to 5.9 km offshore. At the shore the mean wind during this time was from 280-290° at 5-10 m s^{-1} and the air temperature was -20° C. The open-cells range in horizontal size from about 100 m at 1 km offshore to about 500 m at 5.9 km offshore.

Perhaps the most interesting VIL observations during Lake-ICE were open-cell patterns in the steam-fog about 5 meters above the surface of the lake on 10 and 13 January 1998. Cold air advection was occurring on both of these days and visual observations confirmed clear skies over the lidar site and steam fog on the surface of the lake. On 10 January the minimum temperature reached -16.7° C at 14 UTC with the wind from 236° at 6.5 m s^{-1}. On 13 January the air temperature dropped to -20° C and the wind was from 280-290° at 5-10 m s^{-1}. The lake water temperature on these days ranged from 3 to 5° C. In this paper we focus on the 13 January case, but we intend to present other cases at the poster.

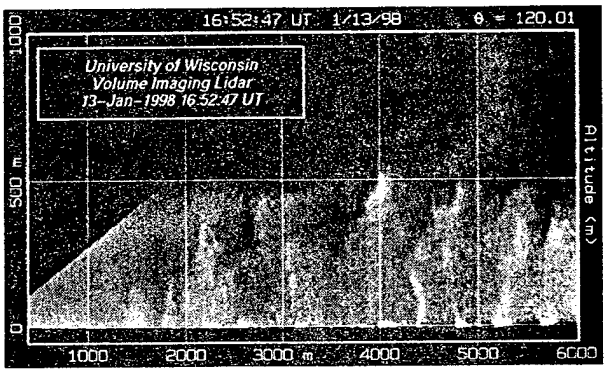

Figure 2. RHI of range-corrected backscatter intensity showing the vertical structure of steam-fog on 13 January 1998 from a couple hundred meters to 6 km offshore. Narrow columns of steam-fog and aerosol can be seen above the lake surface. A 500-m deep mixed layer formed over land appears to be advecting offshore which is also indicated in the upwind radiosonde sounding in figure 3.

The horizontal cell dimensions increase with increasing offshore distance and appear to be slightly elongated in the direction of the wind. Their somewhat hexagonal shape allows any one cell to share most of its walls with neighboring cells. Cell widths on the left side of figure 1 range from approximately 100 to 500 m while cell widths on the right range from 500 to 1000 m. The streaks across the image are caused by attenuation from the steam fog.

While the steam on the 10th did not appear to rise more than about 50-m above the lake, RHI scans from 13 January, such as figure 2, reveal narrow rising columns of steam which sometimes extend to the top of a 500-

m deep mixed-layer. The columns are very bright near the surface and decrease in intensity with altitude. In figure 2, there is one such feature at about 4.4 km range that extends from the surface up to about 200 m. Some of these features may be steam devils and we hope that the VIL observations of them will enable us to quantify their size and number density.

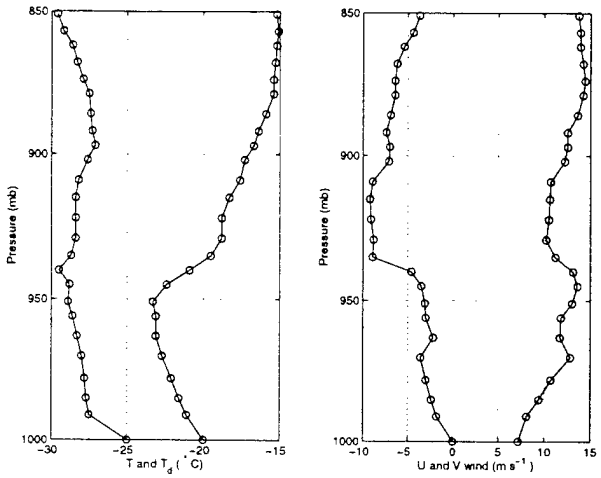

Figure 3. NCAR ISS CLASS sounding from 13 January 1998 at 16:30 GMT was used to initialize our model. The VIL also indicates a mixed layer extending up to about 500 m (about 950 mb) at the coast which is being advected over the lake by the larger scale flow. The wind profile shown here has been rotated so that the surface wind vector is normal to the north-south shoreline in the model.

Modeling

We are running the University of Wisconsin's scalable non-hydrostatic modeling system (Tripoli 1992) to simulate the leading edge of a lake-induced CBL. The model is a computationally efficient, elastic, fully non-Boussinesq grid-point model which includes enstrophy conservation.

For the work presented here, which represents our first attempts to simulate the lake-induced CBL, the model was run three times with horizontal resolutions of 10, 25 and 50 m. All of the simulations used a 0.25 s time-step and a vertical resolution of 1 m at the surface which increased at a rate of 1.1*dz until a resolution of 50 m was obtained (at about 450 m.) All simulations used 140x70x80 grid-points. The surface of the western 40 grid-points of each domain was snow-covered at air-temperature and the remaining surface was water at a temperature of 279 K.

The model was initialized with horizontally homogeneous initial conditions as prescribed by a radiosonde sounding 10 km upwind (figure 3). This profile of temperature, dew point and wind is maintained along the upwind (inflow at western wall) of the domain. Cyclic (periodic) boundary conditions are implemented along the northern and southern walls of the domain. An open boundary condition is maintained along the eastern wall (outflow). A Rayleigh absorbing layer of 16-points with a minimum dissipation time of 10 s was used at the top of the model. For these runs a geostrophic and hydrostatic reference state is assumed. Subgrid-scale turbulence parameterization is a buoyancy enhanced eddy-viscosity closure similar to that of Tripoli and Cotton (1982). Heat, moisture and momentum are transferred from the surface to the lowest layer of the model using standard bulk mixing theory. The model solves for saturation and cloud water diagnostically and the steam fog is produced as the result of supersaturation assuming conservation of total water mixing ratio and entropy.

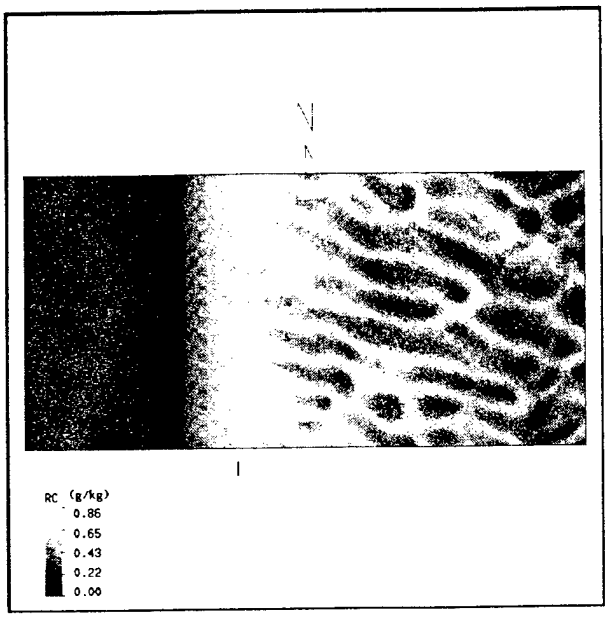

Figure 4. Horizontal distribution of condensed water (steam-fog in g/kg) at the lowest level of the model (1 m) at 30 minutes into simulation. The horizontal grid resolution was 50 m for this run. The size of the domain is 7 km (east-west) by 3.75 km (north-south).

The simulation with 50-m horizontal resolution, which has a horizontal domain of 7.0 by 3.5 km, produces a homogeneous region of steam-fog along the coastline out to approximately 1.5 km offshore where linear rolls form. The image shown in figure 4 is from 30 minutes after the beginning of the simulation—long after parcels entering the upwind edge of the domain would have traversed the full east-west distance of the domain. The flow near the surface veers with increasing offshore distance. At the downwind edge of the domain, the CBL depth has grown to approximately 600 m. When streamlines of the horizontal flow (such as those in figure 6) are superimposed on the condensed water field, the bands of steam-fog lie in regions of convergence and upward motion.

Figure 5 shows an east-west vertical slice of the lowest 15 grid-points at 30 minutes in the simulation. This image ranges from the surface to 26.2 m above the lake and is 7 km wide. The image shows the upward-sloping leading edge of the homogeneous band of steam-fog shown in figure 4 and some narrow columns of steam-fog rising from the surface of the lake. These features, which would be visible wisps of steam fog in reality, can be compared to the very bright spots along the bottom edge of the RHI shown in figure 2. The narrow columns of scattering which sometimes extend to the top of the 500-m deep mixed layer in figure 2 are composed of visible steam fog just above the surface and hygroscopically swollen aerosols at the remaining levels.

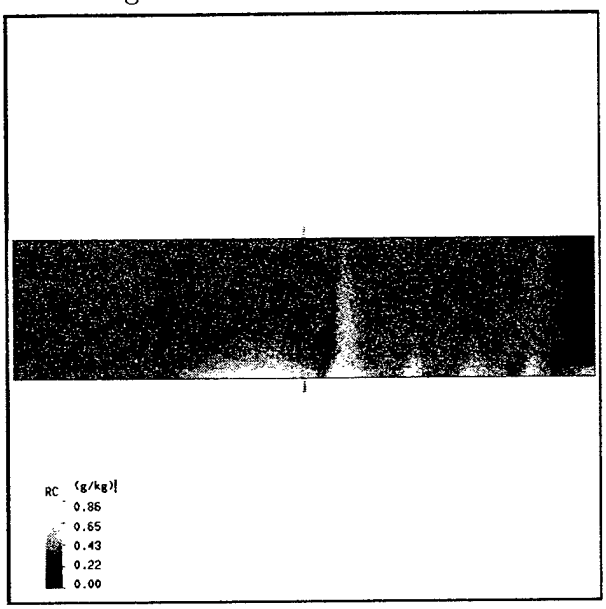

Figure 5. East-west vertical slice through the lowest 15 grid-points of the model domain showing condensed water (steam-fog in g/kg) at 30.0 minutes into simulation. The horizontal grid resolution was 50 m for this run. The image is 7 km wide by 26.2 m tall.

The 25 m and 10 m horizontal resolution simulations also use domains with 140x70x80 grid-points, and thus cover less area than the 50 m grid. The 25 m grid covers 3.5 by 1.75 km and the 10 m grid covers 1.4 km by 700 m. Both of these simulations produce a homogeneous region of steam-fog immediately

downwind of the shoreline followed by linear rolls. Nine roll circulations set up in the 50 m grid (λ = 420 m); approximately 12 in the 25 m grid (λ=160 m), and 18 in the 10 m grid (λ = 40 m). The 50 m grid appears to preserve these roll structures downstream for a much greater proportion of the grid. Downstream of the rolls, a braided or more cellular appearing pattern, can be seen in all three simulations. The dependence of the structure on resolution warrants further investigation.

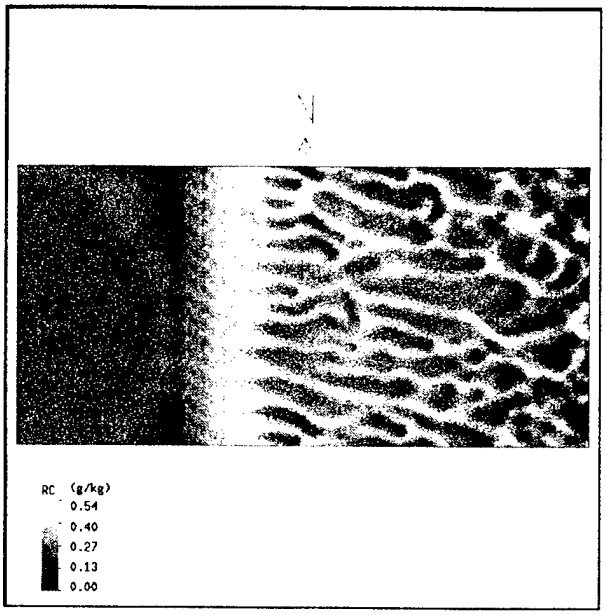

Figure 7. Same as in Figure 4 except with 25 m horizontal resolution and a 3.5 by 1.75 km domain.

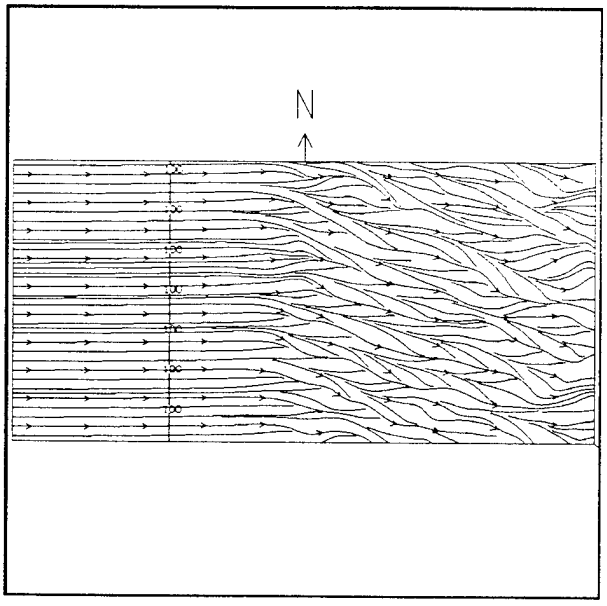

Figure 6. Streamlines of surface wind at 30 minutes into simulation. Grid resolution was 50 m for this run. The vertical line labeled 100 indicates the position of the coastline. This domain is 7 km (east-west) by 3.75 km (north-south).

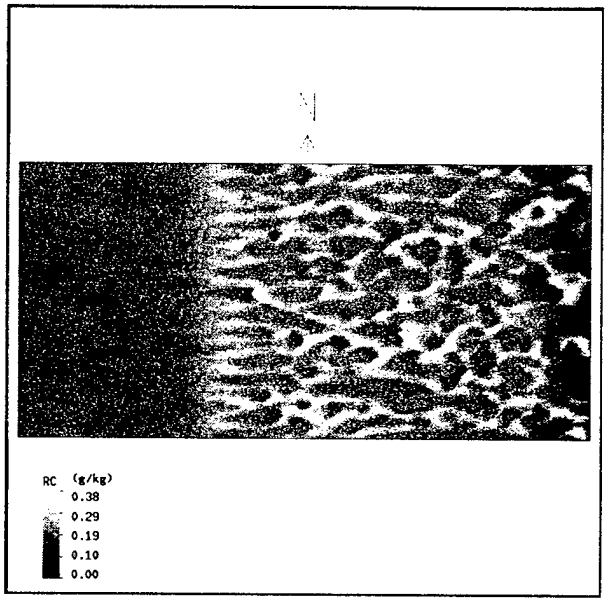

Figure 8. Same as in Figure 4 except with 10 m horizontal resolution and a 1.4 by 0.7 km domain.

All the images shown here are frames extracted from high-resolution color animations. These MPEG movies can be downloaded from our website at http://lidar.ssec.wisc.edu.

Summary

We have begun qualitative comparisons of VIL observations and LES of the lake-induced convective boundary layers. Our next steps include running simulations with high spatial resolution grids and very large domains. We will also perform quantitative comparison of wind fields; boundary layer depth; shapes, sizes and correlation times of the structures in both the observations and model output as a function of offshore distance.

Acknowledgements

This work was made possible by NSF grant number ATM9707165 and ARO grant number ARO DAAH-04-94-G-0195. The calculations were performed on an 8-processor J50 computer furnished by IBM Corporation.

References

Avissar, R., E. W. Eloranta, K. Gurer, G. J. Tripoli, 1998: An Evaluation of the Large-Eddy Simulation Option of the Regional Atmospheric Modeling System in Simulating a Convective Boundary Layer: A FIFE Case Study, *J. Atmos. Sci.*, **55**, 1109–1130.

Eloranta, E. W., 1988: Volume imaging lidar observations of the convective structure surrounding the flight path of a flux-measuring aircraft. *J. Geophys. Res.*, **97**, 18383–18393.

Tripoli, G. J. and W. R. Cotton, 1982: The use of ice-liquid water potential temperature as a thermodynamic variable in deep atmospheric models. *Mon. Wea. Rev.*, **109**, 1094–1102.

Tripoli, G. J., 1992: A nonhydrostatic mesoscale model designed to simulate scale interaction, *Mon. Wea. Rev.*, **120**, 1342–1359.

19th-International Laser Radar Conference
Annapolis, MD, July 6-10, 1998

Lidar Observations of a Land-Breeze Circulation

E. W. Eloranta, R. Kuehn and S. Mayor
University of Wisconsin
1225 W. Dayton Street, Madison, Wisconsin 53706, USA
Phone: 608-262-7327 Fax: 608-262-5974
Email: eloranta@lidar.ssec.wisc.edu

Abstract

Observations of a wintertime land-breeze along the shoreline of Lake Michigan are presented. Sequences of RHI, PPI, and three-dimensional scans with the University of Wisconsin Volume Imaging Lidar provide a detailed description of the flow of cold dense air out over the water in the face of an on-shore synoptic flow. Animations of the lidar data showing the surface outflow, the elevated return flow, gravity waves on the return flow boundary, the fluctuating frontal boundary and the eventual collapse of the front will be presented.

Background

The University of Wisconsin Volume Imaging Lidar (VIL) is designed to provide high spatial and temporal resolution images of atmospheric structure. It employs a Nd:YAG laser operating at a repetition rate of 100 Hz, 0.5-m diameter scanning optics, and a fast data acquisition system to generate two- and three-dimensional images. In typical operation the system records data to a range of 18 km with a range resolution of 15 m. The data system records profiles without averaging. Approximately 1 G-byte of data is recorded per hour of operation.

The VIL was operated as part of the Lake Induced Convection Experiment (Lake-ICE) at a site on the western shore of Lake Michigan from December 5, 1997 to January 19, 1998. Our lidar observations were designed to provide data on convective structures which develop over the lake when cold winter air flows over the unfrozen lake. The strong surface heat flux caused by the air-water temperature difference and the uniform lake surface provide a natural 'laboratory' setting which can be used to test computer models of convection in the atmospheric boundary layer. This paper presents lidar observations of a land-breeze circulation observed between 12:43 UT and 17:12 UT on December 21, 1997. A more complete description of VIL operations during the Lake-ICE experiment is contained in a paper by Mayor *et al.* (these proceedings).

Synoptic Conditions

A large high-pressure system centered northeast of Lake Huron moved slowly eastward during the observation period. The resulting pressure gradient supported a weak southeasterly (on shore) synoptic flow. Figure 1 shows the wind speed and direction measured at the Coast Guard station.

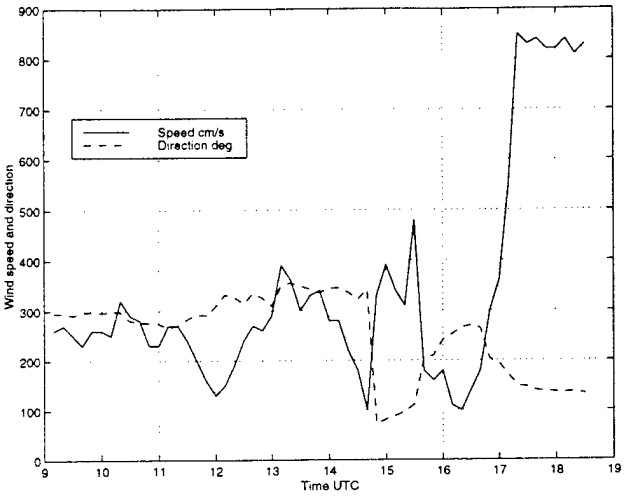

Figure 1. Wind speed and direction measured at the Sheboygan Coast Guard station between 9:00 and 18:30 UTC. The Coast Guard station is located 3/4-km North of the lidar site. Notice that the land-breeze front breaks down at 17:00 UTC under the influence of a weakening land-water temperature differential.

Except for a short period around 15:00 UTC, the offshore flow of the land-breeze is evident from 9:00 to 17:00 UTC. After 17:00 the onshore flow overwhelms the land-breeze flow.

The morning low temperature at the Sheboygan airport ($\sim$ 10 km inland from the lidar) was $-6°$ C and it occurred at 14:00 UTC. The airport temperature rose slowly to $-1°$ C by 17:00 UTC. The morning low temperature at the Sheboygan Coast Guard station (3/4 km north of the lidar on the shore line) was $-3.4°$ C at 11 UTC and the temperature rose to 1.6° C at 18 UTC. NOAA-satellite derived temperatures for the water offshore from the lidar were between 4° and 5° C.

Lidar Observations

Between 12:43 and 13:11 UTC the lidar scanned a three-dimensional volume between azimuth angles of 85° and 135° and elevation angles between 0° and 15°. This scan showed the presence of enhanced scattering close to the lidar and prompted a change in the scan pattern to better image structures near the shore. The new scan began at 13:12 UTC and ended at 15:21 UTC. Each volume scan provided 101 separate RHI scans ($0 - 15°$ elevation) in the azimuth range between 126° and 176°. The volume scan was repeated at intervals of 187 seconds. Figure 2 shows a sample image derived from one of these scans. This image includes one RHI scan along with two constant-altitude cross section created from the same volume scan. Due to the small format available in these proceedings, the horizontal cross sections are enlarged to show only a small portion of the 12-km north-south extent of the lidar images. The 10-m constant altitude scan shows the cold aerosol laden offshore flow in the land-breeze as an aerosol laden region which is roughly parallel to the shoreline of the lake. When a sequence of the 10-m altitude cross sections are animated, motions of the aerosol structures inside the lake-breeze front show a easterly outflow velocity of approximately 2 m/sec. With careful enhancement of this cross section we can also see aerosol inhomogeneities beyond the front. Animation shows an inflow velocity of 5 to 6 m/s from $130 - 140°$ on the lake-side of the front. This is roughly consistent with winds observed at the Coast Guard station after the front collapsed at 17:00 UTC (Fig. 1).

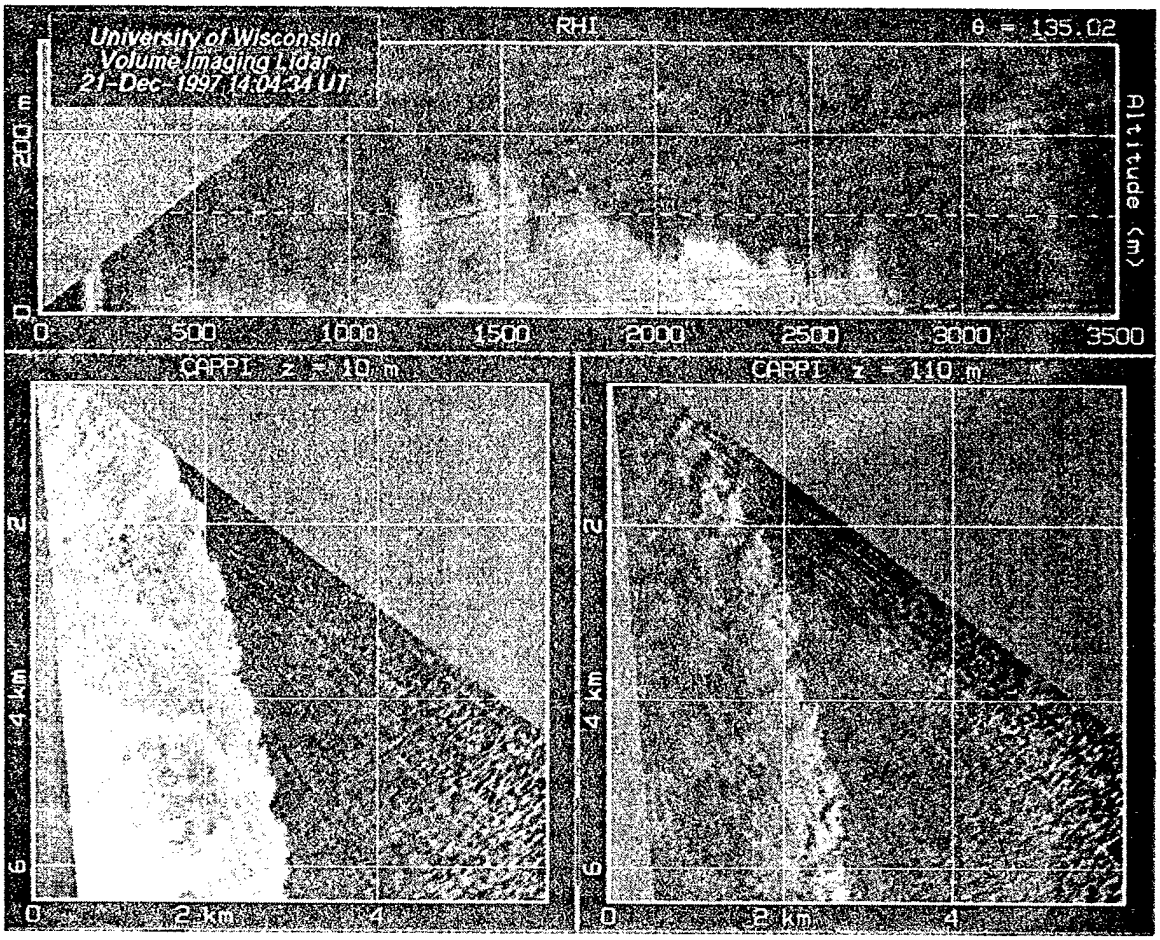

Figure 2. The land-breeze front observed at 14:04 UTC on December 21, 1997. The top panel shows a RHI cross section extending from the surface to an altitude of 300 m and a maximum horizontal range of 3500 m. The RHI is oriented at a compass heading of 134 degrees. The bottom panels show horizontal cross sections over a 6-by 6-km square area at altitudes of 10 m (left) and 110 m (right). North is at the top of the horizontal cross sections and the shoreline runs roughly along the left edge of the images.

The RHI image shows that the front decreases in depth with distance from the shore. It also shows the thin bright land-breeze outflow layer within $\sim$ 20 m of the surface; this is the cold layer of air sliding out over the water against the synoptic flow. Animation of the RHI cross section shows that the land-breeze outflow is confined to a thin layer near the surface. This air appears to flow along the surface to the front where it rises in a strong convergence zone and is then swept back inland in the layer above the outflow. This return flow appears to undergo strong mixing with the marine boundary layer as it is forced up over the land-breeze front. This mixing is evident in the decreased brightness of the upper part of the front near the shore. This decrease of brightness can also be seen in the 110-m cross section which is brightest at the outer edge for the front where air from the surface outflow is being lofted in the convergence zone. Animations show the presence of gravity-wave crests running parallel to the shoreline in the upper part of the front. Point-target-echos also indicate the presence of sea gulls soaring in the air lifted over the

front.

Between 15:24 and 16:46 UTC the lidar was scanned back-and-forth to produce PPI scans at an elevation of 0.06° between an azimuth of 85° and 176°. These were acquired with an angular separation between profiles of 0.08° providing a scan time of 12 seconds. Animations of these scans show the position of the land breeze fluctuating in a series of surges and regressions. The outflow wind is made clearly evident by the motion of aerosol inhomogeneities. The signal strength was sufficient to provide usable images of the front out to a range of approximately 12 km south of the lidar. Visual observations during this period showed the lake to be calm without capillary waves near the shore. Offshore, at a distance which appeared consistent with the lidar imaged front, the water surface turned dark and disturbed by the on shore flow.

Between 16:51 and 17:12 UTC the lidar was programmed to repeatedly repeat an RHI scan between elevations of 0 and 15° with the azimuth held at 165°. The azimuth was selected from visual observations of the cloud motion; the lidar azimuth was set opposite to the wind direction in a newly formed stratocumulus cloud layer. This animation provides vivid images of the return flow even though the images are made more complex by the presence of extremely light snow showers which had begun to fall from an advancing stratocumulus cloud layer. This sequence documents the collapse of the land-breeze front. During the sequence, the frontal surface continuously retreats until it passes over the lidar's shoreline location. Small capillary waves began to build on the water near the shoreline as the front approached. After the frontal passage at 17:00 UTC the water became disturbed. Shortly afterward waves of approximately 30-cm height formed all along the previously calm shoreline.

This presentation will include animations of the lidar observed structure. We also hope to present lidar derived wind profiles in the frontal zone.

Acknowledgments

This research was supported under NSF Grant ATM-9707165 and Army Research Office Grant DAAH04-94-G-0195. Assistance in data acquisition and analysis was provided by P. Ponsardin, J. Hedrick and G. Tubal.

19th-International Laser Radar Conference
Annapolis, MD, July 6-10, 1998

Summary of Volume Imaging Lidar (VIL) Preliminary Results from the Lake-Induced Convection Experiment (Lake-ICE)

Shane D. Mayor, Edwin W. Eloranta, Ralph Kuehn, and Patrick Ponsardin
Department of Atmospheric and Oceanic Sciences, University of Wisconsin
1225 W. Dayton St., Madison, Wisconsin, 53706, USA
phone: 608-263-6847, fax: 608-262-5974, e-mail: shane@lidar.ssec.wisc.edu

Introduction

The University of Wisconsin's Volume Imaging Lidar (UW-VIL) was deployed in Sheboygan, Wisconsin, for the Lake-Induced Convection Experiment (Lake-ICE) during December of 1997 and January of 1998. The site (43°44′N, 87°42′W, 176 m ASL) was located within 10 m of the western shore of Lake Michigan for the purpose of measuring the 4-dimensional (space and time) structure of the upwind edge of the unstable thermal internal boundary layer (TIBL) that forms over the relatively warm lake during cold air outbreaks (CAOs).

Figure 1. Map of the region. For Lake-ICE, the VIL was located in Sheboygan, WI.

During CAOs, the air temperature typically drops to -15 to -30° C while the temperature of the lake water remains a few degrees above freezing. This temperature difference generates large surface heat fluxes which creates a convective boundary layer over the lake. Because the large-scale air flow is from the land to the lake and considering the diffusive nature of turbulence, the TIBL becomes deeper with increasing offshore distance. Stratocumulus clouds form offshore, and steam fog often forms over the lake surface. Futher downwind, the convection can become intense enough to produce lake-effect snow.

Despite the 1997-1998 midwest US winter being one of the mildest on record, we still experienced a few CAOs that were strong enough to enable us to meet our objective. Furthermore, in addition to the TIBLs we observed, we gathered VIL data on many other very interesting phenemona at the edge of the lake, including a land-breeze (see Eloranta *et al.*, this conference), microscale linear and cellular patterns in shallow convection, steam-fog, steam-devils, and gravity waves.

We collected data on 9 days during Lake-ICE, which took place from December 5 until December 22, 1997, and from January 9 until January 22, 1998. The experiment included flights of the NCAR Electra and the University-of-Wyoming King-Air aircraft for in situ boundary layer measurements. Three NCAR integrated sounding systems (ISS) stations and five fixed and one mobile cross-chain loran atmospheric sounding sys-

tem (CLASS) stations provided additional wind and thermodymanic soundings in the surrounding states. The only ISS in Wisconsin was located about 10 km west of the VIL. Measurements of wind and temperature mentioned here are from the National Data Buoy Center's SGNW3 weather station which was located about 750 m north of the VIL. The air temperature and wind were measured at 15.5 m and 19.2 m above the site elevation, respectively.

Motivation

Large eddy simulations (LESs) provide an attractive way of developing parameterizations for large-scale models such as global climate and weather forecast models. This is because they provide 4-D information which can potentially be used to compute fluxes with sampling errors that are much smaller than those made from in situ measurements. LESs, however, are only viable if we have confidence in their solutions. In particular, high resolution 4-D measurements are needed to test the LES.

The UW-VIL is uniquely suited to measure the 4-D structure of aerosol backscatter in the atmospheric boundary layer. By rapidly moving the laser beam in a series of RHIs, each with a slightly increased azimuth angle, we can measure the 3-D structure within a few minutes. For example, a volume which spans 40° in azimuth and 15° in elevation angle requires about 2 minutes and contains about 80 RHIs. The change in elevation angle between two laser pulses during an RHI is 0.23°. By repeating such volume scans, we can also monitor the temporal evolution of the structures. This is possible because the lifetimes of the individual thermals and large-eddies within the boundary layer are long compared to the time it takes to complete one volume scan.

In addition to volume-scans, we also repeated RHI scans at constant azimuths and PPI scans at constant elevations to obtain high temporal resolution 2-D animations of the boundary layer. For example, RHIs (between 0° and 15° elevation) at a constant azimuth direction allow us to produce animations of a vertical slice of the atmosphere with new frames every 2 s. The configuration of the VIL used in Lake-ICE allowed us to transmit 400 mJ/pulse at 100 Hz, and record backscatter intensity at 15-m intervals out to a range of 18 km.

Figure 2. Photograph (looking south) showing the UW-VIL trailer in the foreground on the right and the Edgewater electric power plant in the background on the left. Stack plumes in this photo are blowing to the west.

Interesting observations

Perhaps the most interesting VIL observation during Lake-ICE was open-cell convection patterns in the steam-fog about 5 meters above the surface of the lake on 10 and 13 January 1998. Cold air advection was occurring on both of these days and visual observations confirmed clear skies over the lidar site and steam fog on the surface of the lake. On 10 January the minimum temperature reached -16.7° C at 14 UTC with the wind from 236° at 6.5 m s^{-1}.

The VIL's beam-steering-unit (the point at which lidar beam is transmitted from) was located approximately 5 m above the lake surface. Thus, PPI scans at 0° elevation allowed us to map the horizontal distribution of steam-fog in a plane approximately 5 m above and parallel to the surface of the lake. Figures 3 and 4 are PPI scans of this type. In figure 3, the data range from 5 to 10 km offshore. RHI scans within an hour of this image show that the steam-fog did not rise above ~50 m on this day.

The narrow walls of the cells, where the steam is concentrated, is probably a region of convergence and upward motion with weaker compensating sinking motion in the larger clear interior of the cell. The cells appear to be slightly elongated in the direction of the wind. Their somewhat hexagonal shape allows any one cell to share most of its walls with neighboring cells. The horizontal cell dimensions increase with increasing offshore distance. Cells on the left side of the image range from approximately 200-500 m wide while the cells on the right range from 500-1000 m wide. The streaks across the image are caused by attenuation from the steam fog. On the 10th the fog did not appear to rise more than about 50 m above the lake, while RHI scans from 13 January reveal narrow rising columns of steam which sometimes extend to the top of a 400-m deep mixed-layer. The minimum temperature on the morning of the 13th was -20° C and the wind was from 280-290° at 5-10 m s^{-1}. The columns are very bright near the surface and decrease in intensity with altitude. In figure 5, there is one such feature at about 4.4 km range that extends from the surface up to about 200 m. Some of these features may be steam devils and we hope that the VIL observations of them will enable us to quantify their size and number density.

Figure 3. Enlargement of a 25-km^2 region 5-10 km offshore from a PPI image of range-corrected backscatter intensity. The image shows open-cell organization of convection in the steam-fog over the lake during a cold air outbreak on 10 January 1998. Note the approximately hexagonal shape of the cells. At the shore, the mean wind during this time was from 236° at 6.5 m s^{-1} and the air temperature was -16.7° C. The streaks across the image are caused by attenuation from the steam fog.

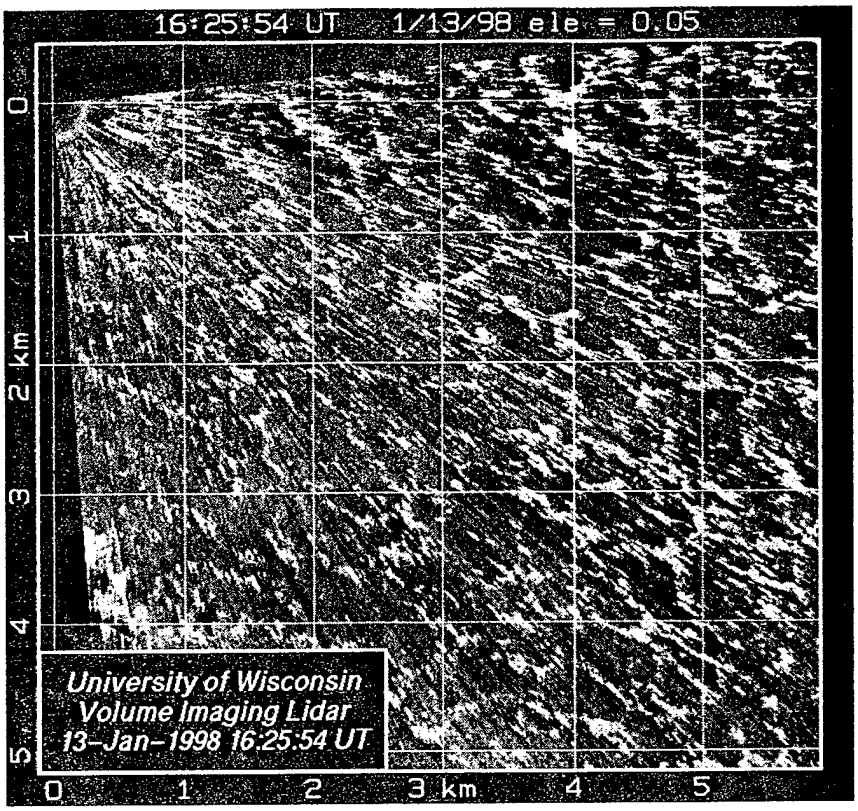

Figure 4. PPI of range-corrected backscatter intensity showing the open-cell organization of the steam fog on 13 January 1998 from a few hundred meters to 5.9 km offshore. At the shore the mean wind during this time was from 280-290° at 5-10 m s^{-1} and the air temperature was -20° C.The open-cells range in horizontal size from about 100 m at 1 km offshore to about 500 m at 5.9 km offshore.

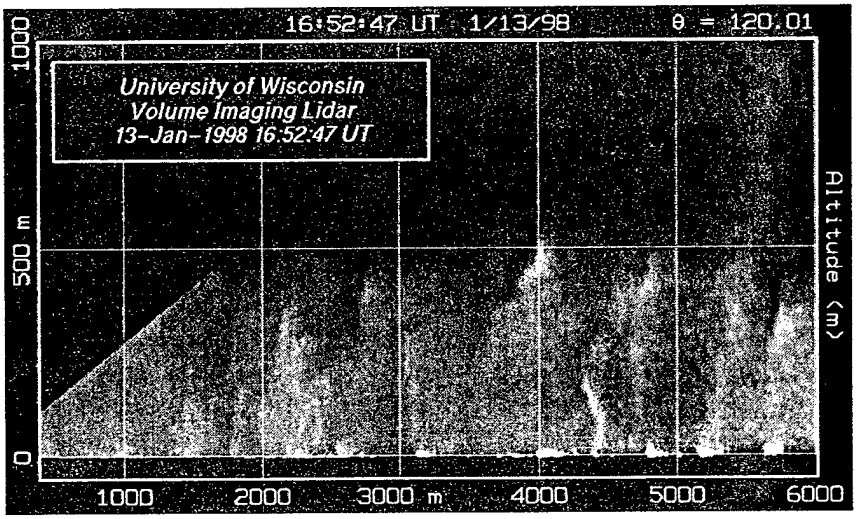

Figure 5. RHI of range-corrected backscatter intensity showing the vertical structure of the steam fog and TIBL over the lake on 13 January 1998.

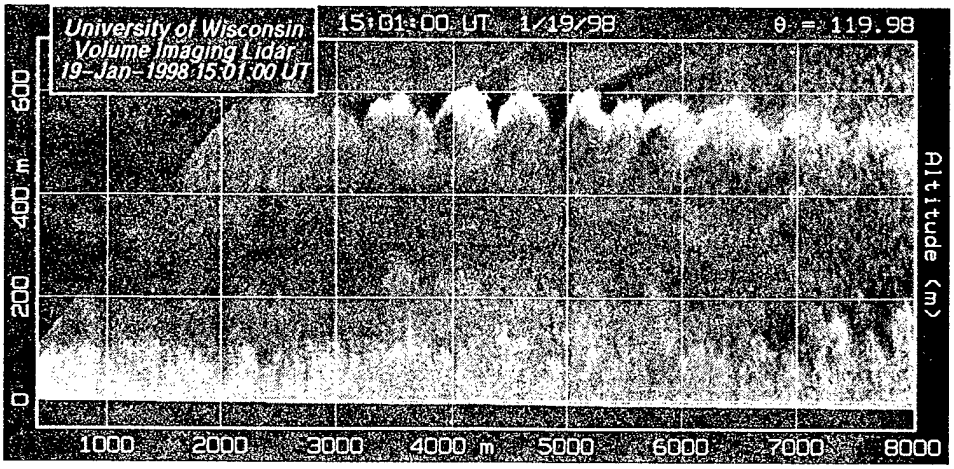

Figure 6. RHI aligned downwind (120° azimuth). This vertical cross-section of the atmosphere over the lake on 19 January 1998 shows gravity waves above a shallow mixed layer.

We saw evidence of lake-induced unstable TIBLs on most of the days we operated the VIL at Lake-ICE. Our first operational day, 5 December 1997, showed a complex boundary layer in which snow caused the air above the TIBL to be higher in scattering than the thermals with origins over the lake.

Figure 6 shows the vertical structure of the lower atmosphere over the lake on 19 January 1998. A shallow mixed layer can be seen from the surface up to about 100 m. A residual layer, or mixed layer produced from the land, which is lower in scattering, can be seen from 100 to 200 m. Gravity waves can be seen between 500 and 600 m above the lake. The waves have an amplitude of approximately 50 m and a wavelength of about 500 m.

On 14 December 1997, we observed a "criss-cross" pattern of waves, or waves and linear convective features, within a 100-km^2 area on PPI displays. The linear features (or waves) with crests that were oriented north-south were moving toward the east and the linear features with crests oriented approximately west-east were moving to the north. The result is a pattern which resembles a "waffle" and is shown in figure 7. The coherent structures are much more obvious in animated color images. The wavelength of both features is 400-500 m. The animation also reveals some counter-clockwise turning of the flow field which may be related to the terrain causing a coastal eddy.

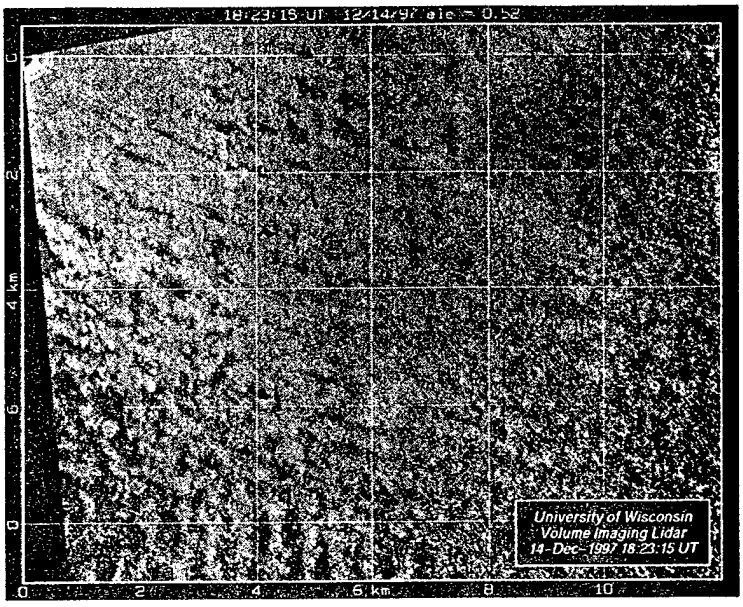

Figure 7. PPI of range-corrected backscatter intensity showing a "criss-cross" of waves or waves and linear coherent structures over the lake on 14 December 1997.

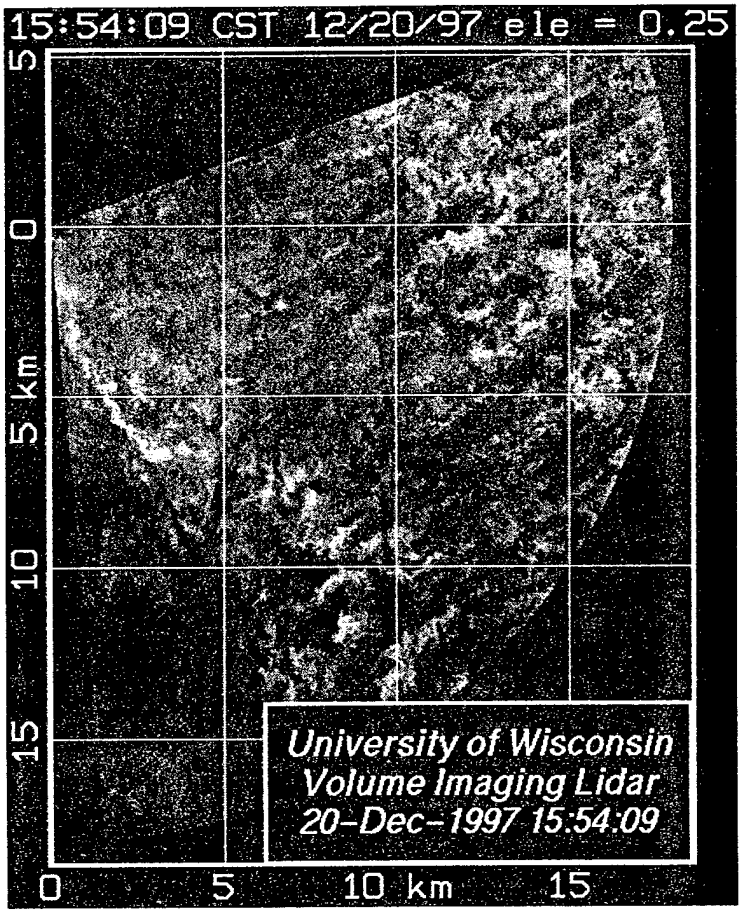

Figure 8. Snow acting as a tracer as it falls into the mixed layer over the lake.

Figure 8 shows patterns in a light snowfall on 20 December 1997. Surface measurements indicated the wind was from 310° at 3-5 m s^{-1} and the air temperature was near 0° C. Animations of the lidar data show structures flowing from the north and a convergence band along a line from approximately 3 km south of the lidar site to a point 5 km east and 10 km south of the lidar. This case was particularly impressive because the signal-to-noise ratio at 18 km was still very high.

While light snow acted as a tracer on a few days, we found the coastal environment near Sheboygan to offer high contrast in the aerosol scattering. Even on days with very high visibility, there was abundant scattering to resolve boundary layer structure. Steam-fog over the lake also provided a high scattering tracer in extremely shallow convection.

All the images shown here are frames extracted from high-resolution color animations. These MPEG movies can be downloaded from our website at http://lidar.ssec.wisc.edu.

Summary

Deployment of the UW-VIL in Lake-ICE during the winter of 97-98 allowed us to collect a rich set of unique measurements of atmospheric boundary layer structures. Our next steps include using the VIL data to quantitatively estimate the shapes of the structures and to compute wind profiles as a function of offshore distance. We also plan to compare these measurements with LES of intense cold-air advection over warm water.

Acknowledgments

This work was made possible by NSF grant number ATM9707165 and ARO grant number ARO DAAH-04-94-G-0195. Thanks to Jim Hedrick and Toby Schwalbe for preparation and maintance of the lidar.

4th International Symposium on Tropospheric Profiling
Snowmass, CO, Sept 20-25, 1998

Volume Imaging Lidar Observations of Atmospheric Boundary Layer Structure over the western edge of Lake Michigan

Ed Eloranta, Shane Mayor, Ralph Kuehn, Patrick Ponsardin, and Jim Hedrick
University of Wisconsin
1225 W. Dayton St., Madison, WI 53706, US

Abstract

We present measurements made by the University of Wisconsin's Volume Imaging Lidar (VIL) during the Dec 97-Jan 98 Lake-Induced Convection Experiment (Lake-ICE). The VIL was located at the edge of Lake Michigan in the city of Sheboygan, Wisconsin, to observe the 4-D structure of convection produced in cold air flowing over the relatively warm lake. Unique VIL observations include the organization of convection within meters of the lake surface, a land-breeze, and thermal internal boundary layers. These data will be analyzed to provide information on the size, shape and orientation of convective eddies along with vertical profiles of wind, and estimates of the horizontal divergence. These measurements will be used to test a Large Eddy Simulation model.

The University of Wisconsin Volume Imaging Lidar (VIL) is designed to provide high spatial and temporal resolution images of atmospheric structure. It employs a Nd:YAG laser operating at a repetition rate of 100 Hz, 0.5-m diameter scanning optics, and a fast data acquisition system to generate two- and three-dimensional images. In typical operation the system records data to a range of 18 km with a range resolution of 15 m. The data system records profiles without averaging. Approximately 1 G-byte of data is recorded per hour of operation.

The VIL was operated as part of the Lake Induced Convection Experiment (Lake-ICE) at a site on the western shore of Lake Michigan from December 5, 1997 to January 19, 1998. Our lidar observations were designed to provide data on convective structures which develop over the lake when cold winter air flows over the unfrozen lake. The strong surface heat flux caused by the air-water temperature difference and the uniform lake surface provide a natural 'laboratory' setting which can be used to test computer models of convection in the atmospheric boundary layer. This paper presents lidar observations of a

Acknowledgements

National Science Foundation Grant ATM-9707165, and by Army Research Office Grant DAAH04-94-G-0022.